Phenomenology of inclusive $\bar{B} \to X_s \ell^+ \ell^-$ for the Belle II era

Tobias Huber,[a] Tobias Hurth,[b] Jack Jenkins,[c] Enrico Lunghi,[c] Qin Qin[d,1] and K. Keri Vos[e]

[a] *Theoretische Physik 1, Naturwissenschaftlich-Technische Fakultät, Universität Siegen,*
Walter-Flex-Straße 3, D-57068 Siegen, Germany

[b] *PRISMA+ Cluster of Excellence and Institute for Physics (THEP),*
Johannes Gutenberg University,
Staudingerweg 9, D-55099 Mainz, Germany

[c] *Physics Department, Indiana University,*
727 E. Third St., Bloomington, IN 47405, U.S.A.

[d] *School of Physics, Huazhong University of Science and Technology,*
Luoyulu 1037, Wuhan 430074, China

[e] *Physics Department T31, Technische Universität München,*
James Franck-Straße 1, D-85748 Garching, Germany

E-mail: huber@physik.uni-siegen.de, tobias.hurth@cern.ch,
jackjenk@iu.edu, elunghi@indiana.edu, qqin@hust.edu.cn,
keri.vos@tum.de

ABSTRACT: With the first data being recorded at Belle II, we are at the brink of a new era in quark flavour physics. The many exciting new opportunities for Belle II include a full angular analysis of inclusive $\bar{B} \to X_s \ell^+ \ell^-$ which has the potential to reveal new physics, in particular by its interplay with the exclusive $b \to s \ell^+ \ell^-$ counterparts studied extensively at LHCb. In this paper, we present fully updated Standard Model predictions for all angular observables necessary for this endeavour. These predictions are tailored to Belle II and include an elaborate study of the treatment of collinear photons which become crucial when aiming for the highest precision. In addition, we present a phenomenological study of the potential for Belle II to reveal possible new physics in the inclusive decay channel, both in an independent manner and in combination with exclusive modes.

---

[1]Corresponding author.

Contents

1 Introduction

Many of the yet unanswered questions of particle physics are related to the Yukawa sector of the Standard Model (SM). In the past decades, flavour physics experiments at electron-positron [1] and hadron machines have already revealed much of our current understanding of the quark sector. With Run-2 data from the LHC being analysed and Belle II having the first dozens of inverse femtobarns on tape, the quark sector of the SM is currently being

investigated to unprecedented precision, possibly revealing and quantifying the remaining mysteries in this sector. Flavour-changing neutral current (FCNC) decays of heavy quarks are among the prime candidates to further scrutinize the quark flavour sector of the SM and to search for physics beyond it. While exclusive decays of B and B_s mesons such as $\bar{B} \to K^{(*)}\ell^+\ell^-$ have played a major role in the experimental programs [2–10] and have revealed certain interesting tensions between experimental data and SM predictions [11–20], inclusive channels such as $\bar{B} \to X_s\ell^+\ell^-$ will be analysed at Belle II, where a full angular analysis is expected to become feasible for the first time [21]. Taken together, the experiments at hadron and electron-positron machines have a huge potential in tackling fundamental questions of particle physics and searching for new phenomena.

On the theoretical side, the description of inclusive $\bar{B} \to X_s\ell^+\ell^-$ is already very much advanced. The short-distance partonic rate is known to NLO [22, 23] and NNLO [24–37] in QCD, and to NLO in QED [38–40]. Recently, also CKM suppressed contributions from multi-particle final states at leading power have become available analytically [41]. In addition, local power-corrections that scale as $1/m_b^2$ [42–45] and $1/m_b^3$ [46, 47] have been analysed. Other long-distance effects stem from intermediate charmonium resonances — most prominently J/ψ and $\psi(2S)$ — which show up as large peaks in the dilepton invariant mass spectrum. Their effect in the low- and high-q^2 regions[1] is treated via the Krüger-Sehgal (KS) approach [48, 49], which has been refined and improved in several respects in [50].

In addition, there are the so-called resolved contributions, which describe nonlocal power corrections arising from operators in the effective field theory other than the ones proportional to $(\bar{s}\Gamma_1 b)(\bar{\ell}\Gamma_2\ell)$. In the low-$q^2$ region, the resolved contributions can be systematically computed using soft-collinear effective theory (SCET) at subleading power [51–53], while in the high-q^2 region the dominating terms (nonfactorizable $c\bar{c}$ contributions) can be re-expanded in local operators and treated along the lines of [54, 55].

Over the years, additional observables have been proposed besides the traditionally studied decay rate and forward-backward asymmetry. In [56] the full set of independent angular observables was identified. Furthermore, it was proposed in [47] to normalise the $\bar{B} \to X_s\ell^+\ell^-$ rate in the high-q^2 region to the inclusive semi-leptonic $\bar{B}^0 \to X_u\ell\nu$ rate *with the same dilepton mass cut* in order to tame the $\mathcal{O}(30-40\%)$ uncertainty coming from poorly known HQET matrix elements at orders $1/m_b^2$ and $1/m_b^3$. This behavior was indeed confirmed in subsequent phenomenological analyses [39, 40, 50], including the present work.

Since it will still take some time until a fully inclusive measurement using the recoil technique will become feasible at Belle II, one has to rely on the sum-over-exclusive method which requires a cut on the hadronic invariant mass M_X to remove $b \to c(\to s\ell\nu)\ell\nu$ charged-current semi-leptonic and other sources of background at Belle II. The effect of an M_X cut in $\bar{B} \to X_s\ell^+\ell^-$, including the sensitivity to sub-leading shape functions, was analysed in [57–59], with certain problems about the SCET scaling of the virtual photon in the low-q^2 region indicated in [51, 52, 60]. In the present work our predictions are given without a hadronic mass cut, leaving such a study for future work.

---

[1]q^2 denotes the dilepton invariant mass squared.

The novelties of the present article are still manifold and tailored to the Belle II era. First, we update the SM predictions of all angular observables, integrated over two bins in the low-q^2 region. For selected observables, the high-q^2 integrated results are also provided. Depending on the observable and the q^2-bin, the updated central values differ by several percent from those of the previous numerical analysis in [40]. The main reasons for this behaviour can be traced back to updated input parameters and the more sophisticated treatment of non-perturbative effects, coming for instance from resonances treated via the Krüger-Sehgal approach as developed in [50]. To probe effects of lepton-flavour violation, we give predictions for R_{X_s}, the inclusive analogue of $R_{K^{(*)}}$, for the first time. Second, we perform a new Monte Carlo study on the treatment of collinear photon radiation tailored to the treatment of collinear photons at Belle II, including the effect of bin migration from the charmonium resonances into the perturbative low-q^2 window. Third, we carry out a comprehensive model-independent new-physics analysis which also considers a study of the synergy and complementarity between inclusive and exclusive $b \to s\ell^+\ell^-$ transitions with the full Belle II data set. Thus, our new analysis paves the road for a full phenomenological study of $\bar{B} \to X_s\,\ell^+\ell^-$ at Belle II.

This article is organised as follows: in section 2 we define all $\bar{B} \to X_s\,\ell^+\ell^-$ observables under consideration, while section 3 contains the phenomenological results of the main observables. In section 4 we describe the treatment of collinear photons and quantify resulting corrections. In section 5 we carry out our comprehensive model-independent new-physics analysis. We conclude in section 6. The paper is supplemented by two appendices. Appendix A contains the SM predictions for the remaining observables relegated from section 3, while we collect new-physics formulas in terms of high-scale Wilson coefficients in appendix B.

2 Definition of the observables

We start from the double-differential decay width $d^2\Gamma/dq^2/dz$, where $z = \cos\theta$ and θ is the angle between the three-momenta of the positively charged lepton and the decaying B meson in the dilepton center-of-mass frame. The differential decay width $d\Gamma_{\ell\ell}/dq^2$ and the unnormalized differential forward-backward asymmetry $dA_{\mathrm{FB}}^{\ell\ell}/dq^2$ for the $\ell = e$ or $\ell = \mu$ final state are then defined as

$$\frac{d\Gamma_{\ell\ell}}{dq^2} \equiv \int_{-1}^{+1} dz\, \frac{d^2\Gamma(\bar{B} \to X_s\ell\ell)}{dq^2 dz} \,, \tag{2.1}$$

$$\frac{dA_{\mathrm{FB}}^{\ell\ell}}{dq^2} \equiv \int_{-1}^{+1} dz\, \frac{d^2\Gamma(\bar{B} \to X_s\ell\ell)}{dq^2 dz} \,\mathrm{sign}(z) \,. \tag{2.2}$$

The normalized forward-backward asymmetry $\overline{A}_{\mathrm{FB}}$ integrated in a region $q_m^2 < q^2 < q_M^2$ (in units of GeV^2) is then given by

$$\overline{A}_{\mathrm{FB}}[q_m^2, q_M^2]_{\ell\ell} \equiv \frac{\int_{q_m^2}^{q_M^2} dq^2 (dA_{\mathrm{FB}}^{\ell\ell}/dq^2)}{\int_{q_m^2}^{q_M^2} dq^2 (d\Gamma_{\ell\ell}/dq^2)} \,. \tag{2.3}$$

In the absence of QED corrections the double-differential decay width $d^2\Gamma/dq^2/dz$ is a second order polynomial in z, giving rise to three independent angular-distribution observables $H_I^{\ell\ell}(q^2)$, $I = T, A, L$ [56]. As pointed out in [40], QED corrections lead to a distortion of the simple polynomial z dependence and result in a complicated function of z. It is therefore instructive to use projections with weight functions $W_I(z)$ to define the $H_I^{\ell\ell}(q^2)$. In the absence of QED corrections the original definitions from [56] are restored, but the use of the weight functions better captures the effects of QED radiation in the angular observables. In addition, the weight functions will give us the flexibility to define further observables, as we will demonstrate below. We therefore define

$$H_I^{\ell\ell}(q^2) = \int_{-1}^{+1} dz \, \frac{d^2\Gamma(\bar{B} \to X_s\ell\ell)}{dq^2 dz} \, W_I(z) \,,$$
$$H_I[q_m^2, q_M^2]_{\ell\ell} = \int_{q_m^2}^{q_M^2} dq^2 \, H_I^{\ell\ell}(q^2) \,. \tag{2.4}$$

Almost all weight functions $W_I(z)$ are constructed from Legendre polynomials $P_n(z)$, which are orthogonal on $z \in [-1, 1]$. Moreover, we can use Legendre polynomials with $n > 2$ to define observables which vanish in the absence of QED corrections. We do this by defining $H_3^{\ell\ell}(q^2)$ and $H_4^{\ell\ell}(q^2)$ for $n = 3$ and $n = 4$, respectively, to get a handle on even and odd powers of z. This leads to the following weight functions,

$$W_T = \frac{2}{3} \, P_0(z) + \frac{10}{3} \, P_2(z) \,, \qquad W_3 = P_3(z) \,,$$
$$W_L = \frac{1}{3} \, P_0(z) - \frac{10}{3} \, P_2(z) \,, \qquad W_4 = P_4(z) \,, \tag{2.5}$$
$$W_A = \frac{4}{3} \text{sign}(z) \,.$$

The differential rate and unnormalized forward-backward asymmetry are related to the angular-distribution observables via

$$\frac{d\Gamma_{\ell\ell}}{dq^2} = H_T^{\ell\ell}(q^2) + H_L^{\ell\ell}(q^2) \,, \qquad \frac{dA_{\text{FB}}^{\ell\ell}}{dq^2} = \frac{3}{4} H_A^{\ell\ell}(q^2) \,. \tag{2.6}$$

The observables $\mathcal{H}_I$ differ from the H_I merely by a normalization which can be deduced from eqs. (4.4) and (4.6) of [40]. To the latter paper we also refer for master formulas of all observables. Our operator basis is the same as in [38]. Finally, the branching ratio is calculated via

$$\mathcal{B}[q_m^2, q_M^2]_{\ell\ell} = \mathcal{H}_T[q_m^2, q_M^2]_{\ell\ell} + \mathcal{H}_L[q_m^2, q_M^2]_{\ell\ell}. \tag{2.7}$$

In the high-q^2 region, we also consider the ratio [47]

$$\mathcal{R}(s_0)_{\ell\ell} = \int_{\hat{s}_0}^1 d\hat{s} \, \frac{d\Gamma_{\ell\ell}}{d\hat{s}} \, \Big/ \, \int_{\hat{s}_0}^1 d\hat{s} \, \frac{d\Gamma(\bar{B}^0 \to X_u\ell\nu)}{d\hat{s}} \,, \tag{2.8}$$

where $\hat{s} = q^2/m_{b,\text{pole}}^2$. The ratio $\mathcal{R}(14.4)_{\ell\ell}$ significantly reduces the uncertainties introduced by hadronic power corrections, which dominate the uncertainties of the high-q^2 $\bar{B} \to X_s\ell^+\ell^-$ decay rate.

Moreover, to quantify the effects of lepton-flavour universality violation in the inclusive $\bar{B} \to X_s \ell^+ \ell^-$ decay, we define the ratio of the decay widths of the muon- to electron-modes

$$R_{X_s}[q_m^2, q_M^2] \equiv \int_{q_m^2}^{q_M^2} dq^2 \frac{d\Gamma_{\mu\mu}}{dq^2} \Big/ \int_{q_m^2}^{q_M^2} dq^2 \frac{d\Gamma_{ee}}{dq^2} \,, \tag{2.9}$$

analogous to the ratios $R_{K^{(*)}}$ in the exclusive channels. Besides, the corresponding ratios for the angular observables H_I ($I = T, A, L$) are also calculated. They are defined by

$$R_{H_I}[q_m^2, q_M^2] \equiv H_I[q_m^2, q_M^2]_{\mu\mu} \Big/ H_I[q_m^2, q_M^2]_{ee} \,. \tag{2.10}$$

3 Phenomenological results

For the updated numerical analysis we use the same input parameters as in our $\bar{B} \to X_d \ell^+ \ell^-$ analysis [50]. They are presented in table 1. The most significant changes compared to the previous $\bar{B} \to X_s \ell^+ \ell^-$ analysis [40] are, on the one hand, the inclusion of the resolved photon contributions [51–53], which we discussed in detail in [50]. Moreover, we implemented the new and more sophisticated treatment of the non-perturbative effects following the Krüger-Sehgal approach [50]. Finally, in the high-q^2 region, the HQET matrix elements λ_2, ρ_1 and the weak annihilation matrix elements $f_u^0, f_u^\pm$ and f_s play a crucial role. We have updated these parameters as discussed in [50] and give their explicit values in table 1. Here the weak annihilation matrix elements are defined as[2]

$$f_q^a \equiv \frac{4\pi^2}{2m_B} \langle B^a | Q_1^q - Q_2^q | B^a \rangle \,, \qquad f_q \equiv (f_q^0 + f_q^\pm)/2 \,, \tag{3.1}$$

where $Q_1^q = \bar{h}_v \gamma_\mu (1 - \gamma_5) q \ \bar{q} \gamma^\mu (1 - \gamma_5) h_v$ and $Q_2^q = \bar{h}_v (1 - \gamma_5) q \ \bar{q}(1 + \gamma_5) h_v$ [61], and $a = 0, \pm$ denotes the charge of the meson. Taking into account isospin and flavour SU(3) considerations, we can rewrite the weak annihilation matrix elements in terms of the valence f_V and non-valence f_{NV} ones. The observables depend on

$$\mathcal{B}(\bar{B} \to X_s \ell^+ \ell^-) \Longrightarrow \begin{cases} f_s = f_{NV} \\ f_u = (f_V + f_{NV})/2 \,, \end{cases} \tag{3.2}$$

$$\mathcal{R}(s_0, \bar{B} \to X_s \ell^+ \ell^-) \Longrightarrow \begin{cases} (f_s + f_u^0)/2 = f_{NV} \\ f_s - f_u^0 = [\delta f]_{SU(3)} \,. \end{cases} \tag{3.3}$$

The input parameters in table 1 are obtained from a re-analysis of [62, 63]. For the ratio $\mathcal{R}(s_0, \bar{B} \to X_s \ell^+ \ell^-)$, the symmetry breaking corrections play an important role. Following ref. [47], we estimated these effects as $[\delta f]_{SU(3)} = 0.04$ and $[\delta f]_{SU(2)} = 0.004$, respectively. In the remainder of this section, we present updated numerical results for the branching ratio in two bins of the low dilepton mass region $1 \, \text{GeV}^2 < q^2 < 6 \, \text{GeV}^2$ and the high dilepton mass region $q^2 > 14.4 \, \text{GeV}^2$. In addition, we give the ratios R_{X_s}, $\mathcal{R}(s_0)$ and the forward-backward asymmetry. The remaining angular observables $\mathcal{H}_T, \mathcal{H}_L, \mathcal{H}_A, \mathcal{H}_3, \mathcal{H}_4$

---

[2]This equation corrects (5.5) in [50], where the factor $4\pi^2$ was missing.

$\alpha_s(M_z) = 0.1181(11)$	$m_e = 0.51099895$ MeV
$\alpha_e(M_z) = 1/127.955$	$m_\mu = 105.65837$ MeV
$s_W^2 \equiv \sin^2\theta_W^{\overline{\rm MS}} = 0.2312$	$m_\tau = 1.77686$ GeV
$|V_{ts}^*V_{tb}/V_{cb}|^2 = 0.96403(87)$ [64]	$\overline{m}_c(\overline{m}_c) = 1.275(25)$ GeV
$|V_{ts}^*V_{tb}/V_{ub}|^2 = 123.5(5.3)$ [64]	$m_b^{1S} = 4.691(37)$ GeV [65, 66]
$|V_{td}^*V_{tb}/V_{cb}|^2 = 0.04195(78)$ [64]	$|V_{us}^*V_{ub}/(V_{ts}^*V_{tb})| = 0.02022(44)$ [64]
$|V_{td}^*V_{tb}/V_{ub}|^2 = 5.38(26)$ [64]	$\arg[V_{us}^*V_{ub}/(V_{ts}^*V_{tb})] = 115.3(1.3)^\circ$ [64]
$\mathcal{B}(\bar{B} \to X_c e\bar\nu)_{\rm exp} = 0.1065(16)$ [67]	$|V_{ud}^*V_{ub}/(V_{td}^*V_{tb})| = 0.420(10)$
$m_B = 5.2794$ GeV	$\arg[V_{ud}^*V_{ub}/(V_{td}^*V_{tb})] = -88.3(1.4)^\circ$
$M_Z = 91.1876$ GeV	$m_{t,\rm pole} = 173.1(0.9)$ GeV
$M_W = 80.379$ GeV	$C = 0.568(7)(10)$ [68]
$\mu_b = 5^{+5}_{-2.5}$ GeV	$\mu_0 = 120^{+120}_{-60}$ GeV
$f_{\rm NV} = (0.02 \pm 0.16)$ GeV^3	$\lambda_2^{\rm eff} = 0.130(21)$ GeV^2 [69]
$f_{\rm V} - f_{\rm NV} = (0.041 \pm 0.052)$ GeV^3	$\lambda_1 = -0.267(90)$ GeV^2 [69]
$[\delta f]_{\rm SU(3)} = (0 \pm 0.04)$ GeV^3	$\rho_1 = 0.038(70)$ GeV^3 [69]
$[\delta f]_{\rm SU(2)} = (0 \pm 0.004)$ GeV^3	

Table 1. Numerical inputs used in the phenomenological analysis as in [50], taken from PDG [70] and CKMfitter Group [64].

are relegated to appendix A. The quoted uncertainties are obtained by varying the inputs within their ranges indicated in table 1, where we assume that m_c and C are fully anti-correlated. Moreover, we have added a 5% uncertainty due to the resolved contributions as in [50]. The total uncertainties are obtained by adding the individual ones in quadrature. Our results are summarized in table 2, including also the ratios R_{H_I} ($I = T, L, A$).

3.1 Branching ratio, low-q^2 region

We give the results for the branching ratios integrated over two bins in the low-q^2 region 1 GeV$^2 < q^2 < 6$ GeV^2. As is customary, we present our results for both electron and muon final states separately. For the low-q^2 region, we neglect $1/m_b^3$ corrections.

$$\mathcal{B}[1, 3.5]_{ee} = (9.82 \pm 0.34_{\rm scale} \pm 0.10_{m_t} \pm 0.21_{C,m_c} \pm 0.11_{m_b} \pm 0.04_{\alpha_s} \pm 0.009_{\rm CKM}$$
$$\pm 0.15_{\rm BR_{sl}} \pm 0.06_{\lambda_2} \pm 0.49_{\rm resolved}) \cdot 10^{-7} = (9.82 \pm 0.67) \cdot 10^{-7} . \quad (3.4)$$

$$\mathcal{B}[3.5, 6]_{ee} = (7.98 \pm 0.47_{\rm scale} \pm 0.09_{m_t} \pm 0.19_{C,m_c} \pm 0.09_{m_b} \pm 0.06_{\alpha_s} \pm 0.01_{\rm CKM}$$
$$\pm 0.12_{\rm BR_{sl}} \pm 0.06_{\lambda_2} \pm 0.40_{\rm resolved}) \cdot 10^{-7} = (7.98 \pm 0.67) \cdot 10^{-7} . \quad (3.5)$$

$$\mathcal{B}[1, 6]_{ee} = (17.80 \pm 0.80_{\rm scale} \pm 0.19_{m_t} \pm 0.39_{C,m_c} \pm 0.20_{m_b} \pm 0.10_{\alpha_s} \pm 0.02_{\rm CKM}$$
$$\pm 0.27_{\rm BR_{sl}} \pm 0.12_{\lambda_2} \pm 0.89_{\rm resolved}) \cdot 10^{-7} = (17.80 \pm 1.33) \cdot 10^{-7} . \quad (3.6)$$

q^2 range [GeV^2]	[1, 3.5]	[3.5, 6]	[1, 6]
$\mathcal{B}$	$\begin{matrix} 9.82 \pm 0.67 \\ 9.44 \pm 0.63 \end{matrix} \times 10^{-7}$	$\begin{matrix} 7.98 \pm 0.67 \\ 7.85 \pm 0.66 \end{matrix} \times 10^{-7}$	$\begin{matrix} 17.80 \pm 1.33 \\ 17.29 \pm 1.28 \end{matrix} \times 10^{-7}$
R_{X_s}	0.961 ± 0.004	0.984 ± 0.002	0.971 ± 0.003
$\mathcal{H}_T$	$\begin{matrix} 2.91 \pm 0.22 \\ 2.08 \pm 0.14 \end{matrix} \times 10^{-7}$	$\begin{matrix} 2.51 \pm 0.24 \\ 2.00 \pm 0.20 \end{matrix} \times 10^{-7}$	$\begin{matrix} 5.42 \pm 0.46 \\ 4.08 \pm 0.34 \end{matrix} \times 10^{-7}$
R_{H_T}	0.714 ± 0.013	0.798 ± 0.013	0.753 ± 0.013
$\mathcal{H}_L$	$\begin{matrix} 6.92 \pm 0.50 \\ 7.37 \pm 0.52 \end{matrix} \times 10^{-7}$	$\begin{matrix} 5.43 \pm 0.44 \\ 5.81 \pm 0.47 \end{matrix} \times 10^{-7}$	$\begin{matrix} 12.35 \pm 0.92 \\ 13.18 \pm 0.96 \end{matrix} \times 10^{-7}$
R_{H_L}	1.065 ± 0.006	1.070 ± 0.006	1.067 ± 0.006
$\mathcal{H}_A$	$\begin{matrix} -0.95 \pm 0.08 \\ -1.03 \pm 0.08 \end{matrix} \times 10^{-7}$	$\begin{matrix} 0.91 \pm 0.16 \\ 0.85 \pm 0.16 \end{matrix} \times 10^{-7}$	$\begin{matrix} -0.04 \pm 0.21 \\ -0.18 \pm 0.21 \end{matrix} \times 10^{-7}$
R_{H_A}	1.077 ± 0.008	0.933 ± 0.013	$-$
$\mathcal{H}_3$	$\begin{matrix} 4.14 \pm 0.70 \\ 1.72 \pm 0.29 \end{matrix} \times 10^{-9}$	$\begin{matrix} 5.00 \pm 0.59 \\ 2.08 \pm 0.25 \end{matrix} \times 10^{-9}$	$\begin{matrix} 9.14 \pm 1.29 \\ 3.80 \pm 0.53 \end{matrix} \times 10^{-9}$
$\mathcal{H}_4$	$\begin{matrix} 6.37 \pm 0.67 \\ 2.65 \pm 0.28 \end{matrix} \times 10^{-9}$	$\begin{matrix} 2.24 \pm 0.21 \\ 0.93 \pm 0.09 \end{matrix} \times 10^{-9}$	$\begin{matrix} 8.60 \pm 0.88 \\ 3.58 \pm 0.36 \end{matrix} \times 10^{-9}$
q^2 range [GeV^2]	> 14.4		
$\mathcal{B}$	$\begin{matrix} 2.04 \pm 0.87 \\ 2.38 \pm 0.87 \end{matrix} \times 10^{-7}$		
R_{X_s}	1.17 ± 0.08		
$\mathcal{R}(s_0)$	$\begin{matrix} 21.53 \pm 2.35 \\ 25.33 \pm 1.93 \end{matrix} \times 10^{-4}$		

Table 2. Summary of the numerical results for the different observables. If applicable, the first entry in each row is for electrons, the second for muons.

$$\begin{aligned} \mathcal{B}[1, 3.5]_{\mu\mu} = (&9.44 \pm 0.30_{\text{scale}} \pm 0.10_{m_t} \pm 0.20_{C,m_c} \pm 0.11_{m_b} \pm 0.04_{\alpha_s} \pm 0.009_{\text{CKM}} \\ &\pm 0.14_{\text{BR}_{\text{sl}}} \pm 0.06_{\lambda_2} \pm 0.47_{\text{resolved}}) \cdot 10^{-7} = (9.44 \pm 0.63) \cdot 10^{-7} \,. \end{aligned} \quad (3.7)$$

$$\begin{aligned} \mathcal{B}[3.5, 6]_{\mu\mu} = (&7.85 \pm 0.45_{\text{scale}} \pm 0.09_{m_t} \pm 0.19_{C,m_c} \pm 0.10_{m_b} \pm 0.06_{\alpha_s} \pm 0.01_{\text{CKM}} \\ &\pm 0.12_{\text{BR}_{\text{sl}}} \pm 0.06_{\lambda_2} \pm 0.39_{\text{resolved}}) \cdot 10^{-7} = (7.85 \pm 0.66) \cdot 10^{-7} \,. \end{aligned} \quad (3.8)$$

$$\begin{aligned} \mathcal{B}[1, 6]_{\mu\mu} = (&17.29 \pm 0.76_{\text{scale}} \pm 0.19_{m_t} \pm 0.39_{C,m_c} \pm 0.20_{m_b} \pm 0.09_{\alpha_s} \pm 0.02_{\text{CKM}} \\ &\pm 0.26_{\text{BR}_{\text{sl}}} \pm 0.12_{\lambda_2} \pm 0.86_{\text{resolved}}) \cdot 10^{-7} = (17.29 \pm 1.28) \cdot 10^{-7} \,. \end{aligned} \quad (3.9)$$

These new results are 6–7% larger compared to the previous numerical analysis [40], and have an increased uncertainty. The difference in the central value can partially be traced back to changes in the input parameters (mainly CKM factors and the value of the semilep-

tonic branching ratio). The remaining shift — and in fact the dominant one — stems from the more sophisticated analysis of the non-perturbative effects by updating the Krüger-Sehgal analysis along the lines of [50]. In addition, in the low-q^2 region we do not implement the $1/m_c^2$ effects as in [55] any more, but add in quadrature a 5% uncertainty for the resolved contributions [51–53], a procedure that was already applied in [50]. It shifts the central value only marginally, but is entirely responsible for the increase in uncertainty.

3.2 Branching ratio, high-q^2 region

In the high-q^2 region, $q^2 > 14.4 \text{ GeV}^2$, we find

$$\mathcal{B}[> 14.4]_{ee} = (2.04 \pm 0.28_{\text{scale}} \pm 0.02_{m_t} \pm 0.03_{C,m_c} \pm 0.19_{m_b} \pm 0.002_{\text{CKM}} \pm 0.03_{\text{BR}_{\text{sl}}}$$
$$\pm 0.006_{\alpha_s} \pm 0.13_{\lambda_2} \pm 0.57_{\rho_1} \pm 0.54_{f_{u,s}}) \cdot 10^{-7} = (2.04 \pm 0.87) \cdot 10^{-7}, \quad (3.10)$$

$$\mathcal{B}[> 14.4]_{\mu\mu} = (2.38 \pm 0.27_{\text{scale}} \pm 0.03_{m_t} \pm 0.04_{C,m_c} \pm 0.21_{m_b} \pm 0.002_{\text{CKM}} \pm 0.04_{\text{BR}_{\text{sl}}}$$
$$\pm 0.006_{\alpha_s} \pm 0.12_{\lambda_2} \pm 0.57_{\rho_1} \pm 0.54_{f_{u,s}}) \cdot 10^{-7} = (2.38 \pm 0.87) \cdot 10^{-7}. \quad (3.11)$$

Here the power corrections proportional to $\lambda_{1,2}, \rho_1, f_u^{0,\pm}, f_s$, expanded to linear power in these parameters, are also included. We only quote the combined uncertainty of the weak annihilation parameters $f_{u,s}$ due to their correlation. Compared to the previous analysis in ref. [40], we find an increased uncertainty caused by the power-corrections ρ_1 and $f_{u,s}$.

3.3 The ratio R_{X_s}

With our updated results, we can now also consider the lepton-universality ratio R_{X_s} for the inclusive decays, defined in eq. (2.9). We discuss this ratio again in more detail in section 5.1, where we study the constraints on new physics. For the SM, we find the following predictions,

$$R_{X_s}[1, 3.5] = 0.961 \pm 0.004_{\text{scale}} \pm 3 \times 10^{-5}{}_{m_t} \pm 0.0002_{C,m_c} \pm 0.0004_{m_b}$$
$$\pm 4 \times 10^{-5}{}_{\alpha_s} \pm 8 \times 10^{-5}{}_{\lambda_1} \pm 7 \times 10^{-5}{}_{\lambda_2} = 0.961 \pm 0.004, \quad (3.12)$$

$$R_{X_s}[3.5, 6] = 0.984 \pm 0.001_{\text{scale}} \pm 4 \times 10^{-5}{}_{m_t} \pm 0.0002_{C,m_c} \pm 0.0005_{m_b}$$
$$\pm 2 \times 10^{-5}{}_{\alpha_s} \pm 3 \times 10^{-5}{}_{\lambda_1} \pm 4 \times 10^{-5}{}_{\lambda_2} = 0.984 \pm 0.002, \quad (3.13)$$

$$R_{X_s}[1, 6] = 0.971 \pm 0.003_{\text{scale}} \pm 7 \times 10^{-6}{}_{m_t} \pm 0.0002_{C,m_c} \pm 0.0004_{m_b}$$
$$\pm 3 \times 10^{-6}{}_{\alpha_s} \pm 6 \times 10^{-5}{}_{\lambda_1} \pm 7 \times 10^{-5}{}_{\lambda_2} = 0.971 \pm 0.003, \quad (3.14)$$

$$R_{X_s}[> 14.4] = 1.17 \pm 0.03_{\text{scale}} \pm 0.0003_{m_t} \pm 0.002_{C,m_c} \pm 0.006_{m_b}$$
$$\pm 0.0009_{\alpha_s} \pm 0.01_{\lambda_2} \pm 0.04_{\rho_1} \pm 0.06_{f_{u,s}} = 1.17 \pm 0.08. \quad (3.15)$$

3.4 The ratio $\mathcal{R}(s_0)$

In order to reduce the large uncertainties from power corrections in the high-q^2 region, we compute the ratio $\mathcal{R}(s_0)_{\ell\ell}$ from eq. (2.8). We find

$$\mathcal{R}(14.4)_{ee} = (21.53 \pm 0.54_{\text{scale}} \pm 0.25_{m_t} \pm 0.15_{C,m_c} \pm 0.09_{m_b} \pm 0.06_{\alpha_s} \pm 0.92_{\text{CKM}}$$
$$\pm 0.11_{\lambda_2} \pm 1.38_{\rho_1} \pm 1.54_{f_{u,s}}) \times 10^{-4} = (21.53 \pm 2.35) \times 10^{-4}, \quad (3.16)$$

$$\mathcal{R}(14.4)_{\mu\mu} = (25.33 \pm 0.27_{\text{scale}} \pm 0.29_{m_t} \pm 0.14_{C,m_c} \pm 0.03_{m_b} \pm 0.07_{\alpha_s} \pm 1.09_{\text{CKM}}$$
$$\pm 0.04_{\lambda_2} \pm 0.83_{\rho_1} \pm 1.29_{f_{u,s}}) \times 10^{-4} = (25.33 \pm 1.93) \times 10^{-4}. \quad (3.17)$$

Even though this ratio is much less sensitive to power corrections, the latter contributes significantly to the uncertainty. However, note that the uncertainty has been reduced to about 10%, which is smaller than in previous analysis although we include 30% SU(3) breaking effects in the weak annihilation parameters. This reveals once more the robustness of this ratio.

3.5 Forward-backward asymmetry, low-q^2 region

The forward-backward asymmetry $A_{\rm FB}$ and the related angular observable H_A defined in eqs. (2.2) and (2.4) are computed for the low-q^2 region. These observables have a zero-crossing at a position q_0^2 (in units of GeV^2) which we find to be

$$
\begin{aligned}
(q_0^2)_{ee} = 3.28 &\pm 0.11_{\rm scale} \pm 0.001_{m_t} \pm 0.02_{C,m_c} \pm 0.05_{m_b} \\
&\pm 0.03_{\alpha_s} \pm 0.002_{\lambda_1} \pm 0.001_{\lambda_2} \pm 0.06_{\rm resolved} = 3.28 \pm 0.14 \,,
\end{aligned} \tag{3.18}
$$

$$
\begin{aligned}
(q_0^2)_{\mu\mu} = 3.40 &\pm 0.12_{\rm scale} \pm 0.001_{m_t} \pm 0.02_{C,m_c} \pm 0.05_{m_b} \\
&\pm 0.03_{\alpha_s} \pm 0.002_{\lambda_1} \pm 0.002_{\lambda_2} \pm 0.06_{\rm resolved} = 3.40 \pm 0.15 \,.
\end{aligned} \tag{3.19}
$$

For the normalized forward-backward asymmetry it is natural to subdivide the low-q^2 region into two bins due to the zero-crossing,

$$
\begin{aligned}
\overline{A}_{\rm FB}[1,3.5]_{ee} = (-7.28 &\pm 0.67_{\rm scale} \pm 0.01_{m_t} \pm 0.11_{C,m_c} \pm 0.23_{m_b} \\
&\pm 0.19_{\alpha_s} \pm 0.04_{\lambda_2} \pm 0.51_{\rm resolved})\% = (-7.28 \pm 0.90)\% \,,
\end{aligned} \tag{3.20}
$$

$$
\begin{aligned}
\overline{A}_{\rm FB}[3.5,6]_{ee} = (8.57 &\pm 0.74_{\rm scale} \pm 0.01_{m_t} \pm 0.13_{C,m_c} \pm 0.37_{m_b} \\
&\pm 0.18_{\alpha_s} \pm 0.11_{\lambda_2} \pm 0.60_{\rm resolved})\% = (8.57 \pm 1.05)\% \,,
\end{aligned} \tag{3.21}
$$

$$
\begin{aligned}
\overline{A}_{\rm FB}[1,6]_{ee} = (-0.18 &\pm 0.79_{\rm scale} \pm 0.004_{m_t} \pm 0.13_{C,m_c} \pm 0.30_{m_b} \\
&\pm 0.20_{\alpha_s} \pm 0.02_{\lambda_2} \pm 0.01_{\rm resolved})\% = (-0.18 \pm 0.88)\% \,,
\end{aligned} \tag{3.22}
$$

$$
\begin{aligned}
\overline{A}_{\rm FB}[1,3.5]_{\mu\mu} = (-8.16 &\pm 0.68_{\rm scale} \pm 0.01_{m_t} \pm 0.11_{C,m_c} \pm 0.23_{m_b} \\
&\pm 0.20_{\alpha_s} \pm 0.05_{\lambda_2} \pm 0.57_{\rm resolved})\% = (-8.16 \pm 0.95)\% \,,
\end{aligned} \tag{3.23}
$$

$$
\begin{aligned}
\overline{A}_{\rm FB}[3.5,6]_{\mu\mu} = (8.13 &\pm 0.81_{\rm scale} \pm 0.01_{m_t} \pm 0.13_{C,m_c} \pm 0.39_{m_b} \\
&\pm 0.19_{\alpha_s} \pm 0.11_{\lambda_2} \pm 0.57_{\rm resolved})\% = (8.13 \pm 1.09)\% \,,
\end{aligned} \tag{3.24}
$$

$$
\begin{aligned}
\overline{A}_{\rm FB}[1,6]_{\mu\mu} = (-0.77 &\pm 0.84_{\rm scale} \pm 0.004_{m_t} \pm 0.13_{C,m_c} \pm 0.31_{m_b} \\
&\pm 0.21_{\alpha_s} \pm 0.02_{\lambda_2} \pm 0.05_{\rm resolved})\% = (-0.77 \pm 0.93)\% \,.
\end{aligned} \tag{3.25}
$$

4 Treatment of collinear photons

In our calculation we include the effects of a single photon emission from the final state leptons. In the analytic expressions we derived in [40], the dilepton invariant mass is calculated without the inclusion of the photon, which is therefore considered to be part of the hadronic system. Contributions of photon radiation to the double differential branching ratio $d^2\mathcal{B}/dq^2dz$ are calculated in the collinear approximation. One general result is that collinear radiation effects vanish once the differential rate is integrated over the entire phase space. Effects are only possible for low and high q^2 separately and tend to have opposite

sign. The reason is that the differential branching ratio $d\mathcal{B}/dq^2$ is not an infrared safe quantity with respect to collinear photon radiation off final state leptons. The integrated branching ratio, on the other hand, is infrared safe.

The typical size of the electromagnetic effects is expected to be small (i.e. of the order of $\alpha_e/(4\pi)\log m_b^2/m_e^2 \sim 1\%$). There are, however, instances in which the net effect turns out to be disproportionately large. This is the case for $\mathcal{H}_T$ at low-q^2 for which collinear photon effects are $\mathcal{O}(1)$. We refer to section 7 of ref. [40] for a complete discussion of this point.

In this section we discuss the effects of collinear radiation from the two narrow resonances J/ψ and $\psi(2S)$. Compared to electrons, muons radiate much less due to their larger mass. Moreover, muons can be well separated from collinear photons in the detector, which is why we focus on the electron case in what follows. It is easy to show that the emission of a real photon can only decrease the invariant mass of the dilepton: $(p_{e^+} + p_{e^-})^2 < (p_{e^+} + p_{e^-} + p_{\gamma,\text{coll}})^2$. The net effect is a bin migration of the spectrum towards lower dilepton invariant mass: radiation from the resonances can only effect low-q^2 observables.

Unfortunately, it is impossible to produce a reliable estimate of collinear radiation from J/ψ and $\psi(2S)$. In fact, while we are able to use the KS dispersive approach to achieve a complete description of resonances in the colour singlet channel, there is no accurate theoretical approach for the calculation of the colour octet channel. Using the KS method, the colour singlet contributions to the branching ratios $\bar{B} \to X_s\psi \to X_s e^+e^-$ are found to be 1.1×10^{-4} and 5.9×10^{-6} for the J/ψ and $\psi(2S)$ cases; using the measured branching ratios for direct charmonium production [70] we find 4.7×10^{-4} and 2.4×10^{-5}, respectively. The colour singlet channel accounts for only a quarter of the total resonance contribution: this result is well known. It can be taken into account by adding a corresponding multiplicative factor (also referred to "fudge factors" in the literature) of about 2 to the $\bar{B} \to (J/\psi X_s, \psi(2S) X_s)$ amplitudes. As we discussed at length in section 4 of ref. [50], this problem becomes manageable at low-q^2 where the effects of the colour octet channel are included in the so-called resolved contributions which have been estimated to lead to a level below 5%.

Given our inability to calculate accurately the effects of the two narrow charmonium resonances, it is imperative to make sure that bin migration from the resonances does not pollute the low-q^2 branching ratio above the few percent level. Using Monte Carlo events generated using EVTGEN [71], JETSET [72] and PHOTOS [73] (see section 7 of ref. [40] for a complete description of the event generation), it is straightforward to calculate the contribution of a given bin in q^2 to the integrated low-q^2 branching ratios. The results of this analysis are presented in figure 1, where the blue, red and black curves give the probability of migration into the $[1, 3.5]$ GeV^2, $[3.5, 6]$ GeV^2 and $[1, 6]$ GeV^2 bins. Convoluting these results with the analytical expressions for resonant production (rescaled by the appropriate fudge factor to roughly take into account colour octet effects), we see that the contributions of the J/ψ and $\psi(2S)$ to the low-q^2 branching ratios integrated in the three bins mentioned above can be roughly estimated as $(3, 6, 9) \times 10^{-6}$ and $(1, 1.5, 2.5) \times 10^{-7}$, respectively. In comparison with the results presented in section 3, we see that J/ψ contamination is larger than the non-resonant contribution by almost an order of magnitude (the resonant contributions to the three bins are a factor of 3, 8 and 5 times larger than the non-resonant ones).

The problem discussed in the above paragraph is very well known and has been taken into account in existing experimental analyses. For instance, in the most recent Belle measurement of the low-q^2 branching ratio, the quantity $q^2_{ee\gamma} = m^2_{ee\gamma}$ was formed by including collinear photons (if any) with the leptons. Some of the events with $q^2_{ee\gamma}$ near the J/ψ or $\psi(2S)$ resonances will have q^2_{ee} in the $[1,6]$ GeV^2 range (as we mentioned above, drift is only possible towards lower values of q^2_{ee}). Events with $q^2_{ee\gamma}$ in the ranges $[7.3, 10.5]$ GeV^2 and $[12.5, 14.3]$ GeV^2 were vetoed to suppress backgrounds from bin migration from J/ψ and $\psi(2S)$ respectively.

We investigated the effect of this cut on all low-q^2 observables using events generated in Monte Carlo as follows: for each $\bar{B} \to X_s \ell^+ \ell^-$ event, photons with the ten highest energies in the lab frame were considered in addition to the two lepton momenta. For each photon, if the photon angle was within 50 mrad of $p_+(p_-)$, it was added to a total photon vector $k_+(k_-)$ (in case it was within both cones, there was an addition to the cone of the nearest lepton). If the energy of $k_+(k_-)$ exceeded a threshold of 20 MeV, then it was added to $p_+(p_-)$. The dilepton mass square and angular variable z were then computed with the potentially modified lepton momenta. The results of this study are shown in the "$q^2 = q^2_{ee}$" section of table 3. We also investigated the mild dependence of the cone angle and energy threshold.

Alternatively, the quantity $q^2_{ee\gamma}$ can be used in place of q^2_{ee} to form histograms of observables, circumventing the need to correct for bin migration. However, including collinear photons in the definition of the dilepton momentum no longer corresponds to the definition used to make our theoretical predictions (recall that the photon is treated as part of the hadronic system in the theoretical predictions). In order to make bins in $q^2_{ee\gamma}$ in an experimental analysis and compare them to theoretical predictions, shifts need to be made and can be estimated in Monte Carlo in the same fashion as before (see the "$q^2 = q^2_{ee\gamma}$" section of table 3).

The shifts required for the latter analysis strategy are noticeably larger, in particular for the branching ratio in the high-q^2 region and for $\mathcal{H}_T$. This study suggests that the optimal strategy for dealing with collinear photons at Belle II is to treat all prompt photons as part of the hadronic system. After removing peaking backgrounds from the narrow resonances J/ψ and $\psi(2S)$, the binned observables can be compared directly to our theoretical predictions after applying the appropriate "$q^2 = q^2_{ee}$" correction terms presented in table 3.

5   New physics sensitivities

In this section we discuss the existing constraints that Babar and Belle measurements impose on the Wilson coefficients and the projected sensitivity of Belle II with 50ab^{-1} of integrated luminosity. We assume that the magnetic moment coefficients C_7 and C_8 do not receive appreciable new physics contributions and focus on the semileptonic operators. We express our results in terms of the new physics contributions to the Wilson coefficients evaluated at the matching scale $\mu_0 = 120$ GeV and adopt the parameterization

$$C^\ell_{9,10}(\mu_0) = C^{\ell,\mathrm{SM}}_{9,10} + C^{\ell\mathrm{NP}}_{9,10} \,, \tag{5.1}$$

with $\ell = e, \mu$. Our operator basis is the same as in [38].

			$q^2 = q^2_{ee}$			$q^2 = q^2_{ee\gamma}$
	50 mrad	100 mrad	50 mrad	50 mrad	100 mrad	50 mrad
	20 MeV	20 MeV	80 MeV	20 MeV	20 MeV	80 MeV
$\mathcal{B}[1, 3.5]$	−0.5 %	−0.6 %	−0.5 %	−1.9 %	−2.2 %	−1.8 %
$\mathcal{B}[3.5, 6]$	−1.6 %	−1.9 %	−1.6 %	−1.3 %	−1.4 %	−1.2 %
$\mathcal{B}[1, 6]$	−1.0 %	−1.2 %	−1.0 %	−1.6 %	−1.9 %	−1.5 %
$\mathcal{H}_T[1, 3.5]$	−5.6 %	−6.7 %	−5.6 %	−13.8 %	−16.7 %	−13.5 %
$\mathcal{H}_T[3.5, 6]$	−6.7 %	−8.0 %	−6.7 %	−12.9 %	−15.3 %	−12.5 %
$\mathcal{H}_T[1, 6]$	−6.1 %	−7.3 %	−6.1 %	−13.4 %	−16.1 %	−13.0 %
$\mathcal{H}_L[1, 3.5]$	1.1 %	1.3 %	1.1 %	2.0 %	2.5 %	2.0 %
$\mathcal{H}_L[3.5, 6]$	0.2 %	0.2 %	0.2 %	2.8 %	3.4 %	2.7 %
$\mathcal{H}_L[1, 6]$	0.7 %	0.9 %	0.7 %	2.3 %	2.9 %	2.3 %
$\mathcal{H}_A[1, 3.5]$	0.2 %	0.2 %	0.2 %	2.1 %	2.6 %	2.0 %
$\mathcal{H}_A[3.5, 6]$	−4.7 %	−5.8 %	−4.7 %	−11.6 %	−13.8 %	−10.1 %
$\mathcal{H}_A[1, 6]$	2.6 %	3.3 %	2.6 %	9.0 %	10.9 %	8.2 %
$\mathcal{B}[> 14.4]$	0 %	0 %	0 %	6.4 %	7.4 %	5.9 %

Table 3. Correction factors to the SM predictions presented in section 3 required for a direct comparison with measurements performed using the two experimental strategies $q^2 = q^2_{ee}$ and $q^2_{ee\gamma}$ as defined in the text.

We first consider the existing bounds which stem from branching ratio measurements at low- and high-q^2. The weighted average of the BaBar [74, 75] and Belle [76, 77] experimental results are:

$$\mathcal{B}[1, 6]_{\ell\ell} = (1.58 \pm 0.37) \times 10^{-6} \,, \tag{5.2}$$

$$\mathcal{B}[> 14.4]_{\ell\ell} = (0.48 \pm 0.10) \times 10^{-6} \,, \tag{5.3}$$

where we have averaged over the electron and muon modes as well. We assume that the size of relative error in our theoretical predictions is independent of the Wilson coefficients $C_{9,10}(\mu_0)$. Using the numerical formulae presented in appendix B we present the existing 95% C.L. bounds on $C^{\text{NP}}_{9,10}$ in the left panel of figure 2 where we show separately the constraints from the low- and high-q^2 branching ratio measurements.

In order to determine the constraints that can be achieved with 50 ab^{-1}, we assume SM central values and adopt projected experimental sensitivities obtained by combining the estimates for the branching ratio uncertainties presented in refs. [21, 78] with the method adopted in ref. [40] for $\mathcal{H}_T$ and $\mathcal{H}_L$. In table 4 we present the projected statistical uncertainties we use. The total uncertainties are obtained by adding a 5.8% (3.9%) systematic error to all low-q^2 (high-q^2) observables.

The projected uncertainty on the ratio $\mathcal{R}(14.4)$ requires an estimate of the expected experimental error on the semileptonic $\bar{B} \to X_u \ell \nu$ branching ratio measured with $q^2_{\ell\nu} >$
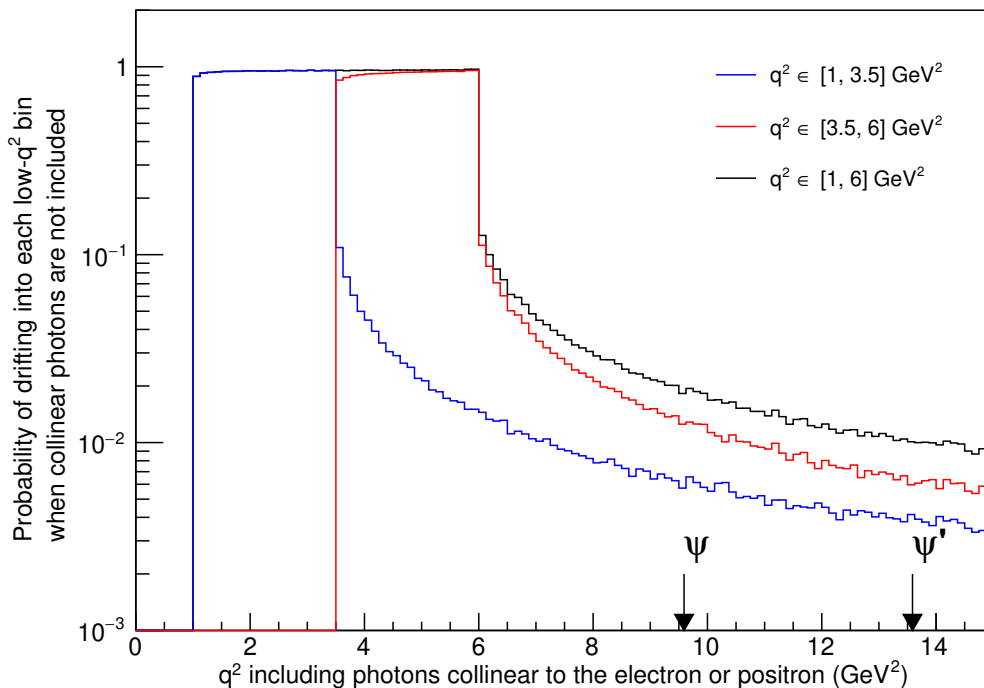
Figure 1. The probability that a $\bar{B} \to X_s \ell^+ \ell^-$ event with photons collinear to either outgoing lepton ($\theta < 50$mrad and $E_\gamma > 20$MeV in the Belle II laboratory frame) will drift into the low-q^2 bin as a result of including only the charged particles in the definition of q^2, using events generated in Monte Carlo. The resonances ψ and ψ' are marked on the horizontal axis.

14.4 GeV^2. We assess the latter by rescaling the expected experimental error on the extraction of $V_{ub}^{\rm incl}$ (see table 59 of ref. [21]) by an estimate of the fraction of the semileptonic spectrum for $q_{\ell\nu}^2 > 14.4$ GeV^2 which we obtained by a sample spectrum presented in ref. [79]. As a rough estimate of this projected uncertainty we find $[\delta\mathcal{R}(14.4)]_{50 \text{ ab}^{-1}}^{\rm exp} = 7.3\%$.

The expected constraints obtained by considering separate measurements of $\mathcal{H}_{T,L,A}$ in the two low-q^2 bins, the high-q^2 branching ratio and the ratio $\mathcal{R}(14.4)$, are presented in the right panel of figure 2. In figure 3 we show the breakdown of the low-q^2 constraints. In particular, we see that considering the two low-q^2 bins separately is mostly relevant for $\mathcal{H}_T$ and especially for $\mathcal{H}_A$. In the two panels of figure 4 we show the relative contribution of low- and high-q^2 observables to the bounds expected. At high-q^2 it is imperative to consider the ratio $\mathcal{R}(14.4)$ in order to reduce exposure to large power corrections which stem from the breakdown of the OPE at the end-point of the spectrum. From the SM results in eqs. (3.16), (3.17) we see that a large fraction of the uncertainty on $\mathcal{R}(14.4)$ is due to the direct determination of $|V_{ub}|$. In figure 5 we show the constraints from the QED observables $\mathcal{H}_{3,4}$.
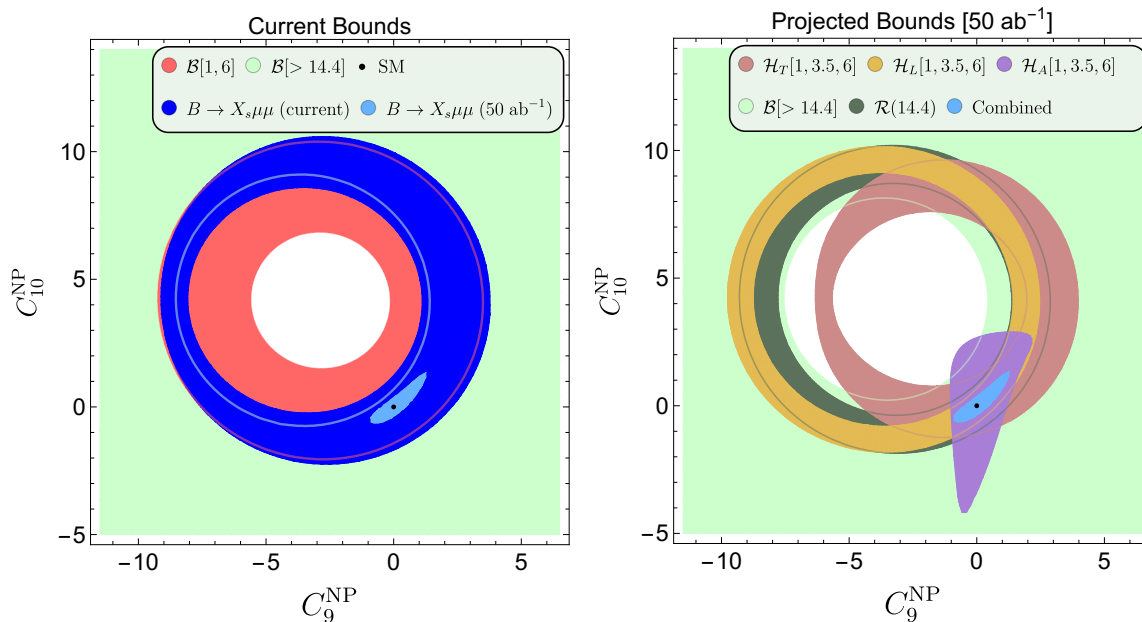
Figure 2. Current (left panel) and expected bounds (right panel) on the new physics contributions to the Wilson coefficients $C_9(\mu_0)$ and $C_{10}(\mu_0)$ with $\mu_0 = 120\,\text{GeV}$. The coefficients $C_{7,8}$ are kept at their SM values. All regions are determined at 95% C.L.. In both panels we combine the electron and muon channels under the assumption $C_{9,10}^e = C_{9,10}^\mu$. In the 50 ab^{-1} extrapolation we combine separately projected measurements of H_T, H_L and H_A in the two low-q^2 bins.

	$[1, 3.5]$	$[3.5, 6]$	$[1, 6]$	> 14.4
$\mathcal{B}$	3.1 %	2.6 %	2.0 %	2.6%
$\mathcal{H}_T$	24 %	15 %	13 %	—
$\mathcal{H}_L$	5.5 %	5.0 %	3.7 %	—
$\mathcal{H}_A$	40 %	33 %	— %	—
$\mathcal{H}_3$	240 %	140 %	120 %	—
$\mathcal{H}_4$	140 %	270 %	120 %	—

Table 4. Projected statistical uncertainties that we expect at Belle II with 50 ab^{-1} of integrated luminosity. The first row gives the considered q^2 bin in GeV^2. The total projected error is obtained by adding a 5.8(3.9)% systematic uncertainty to all low-q^2 (high-q^2) observables.

5.1 Interplay between inclusive and exclusive decays

In this subsection we discuss the interplay between the experimental projections we discussed above and the existing anomalies in exclusive modes. Since some of the latter (such as P_5') are specific to the di-muon final state, and since modifying only the muonic Wilson coefficients can already accommodate the data, we present bounds in the $[C_9^{\mu\text{NP}}, C_{10}^{\mu\text{NP}}]$ plane, assuming there are no new physics contributions to the coefficients $C_{9,10}^e$.
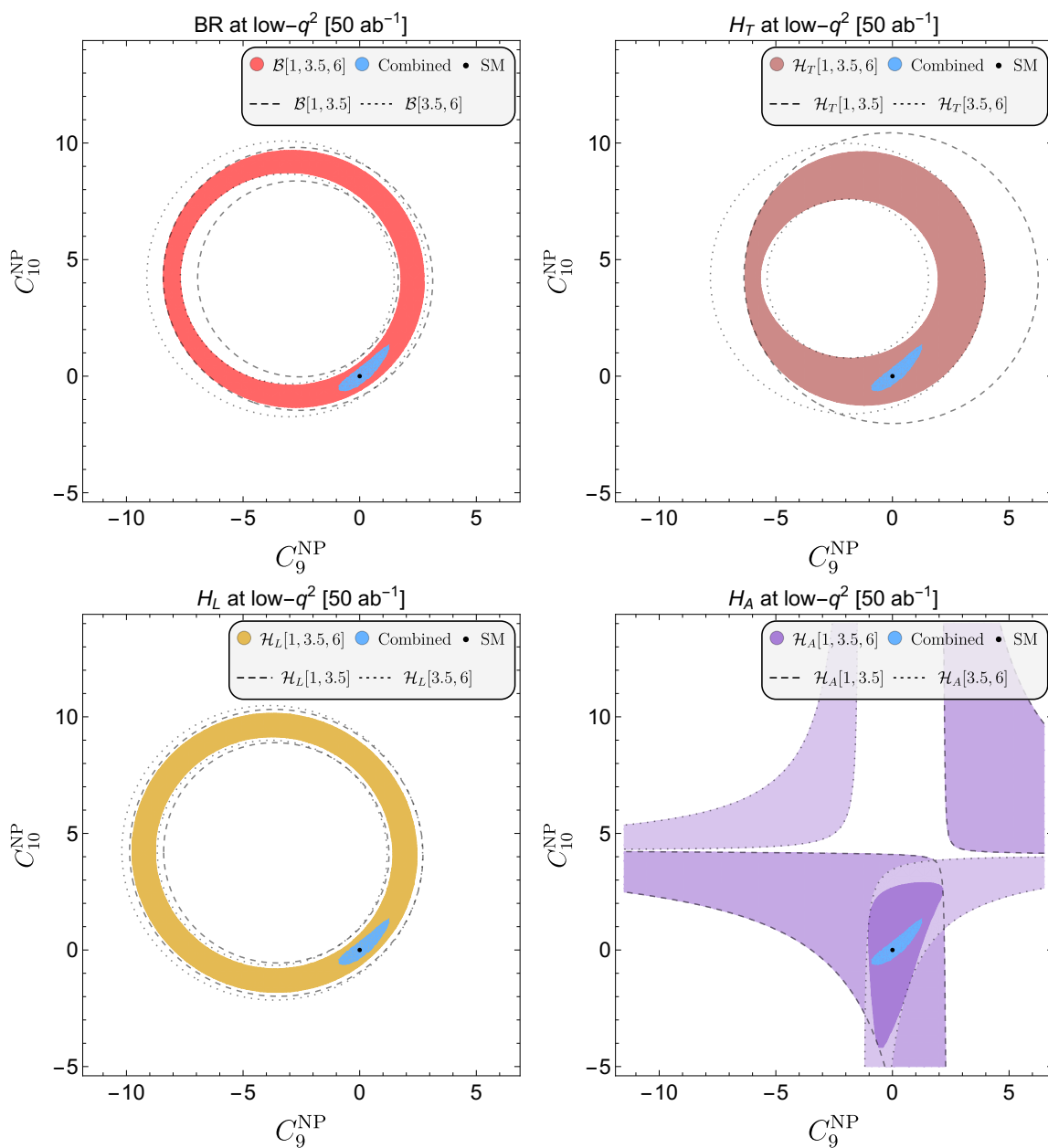
Figure 3. Bounds from individual measurements of low-q^2 branching ratio, $\mathcal{H}_T$, $\mathcal{H}_L$ and $\mathcal{H}_A$. In each case we show the constraints from the two low-q^2 bins and from their combination. See the caption in figure 2 for further details.
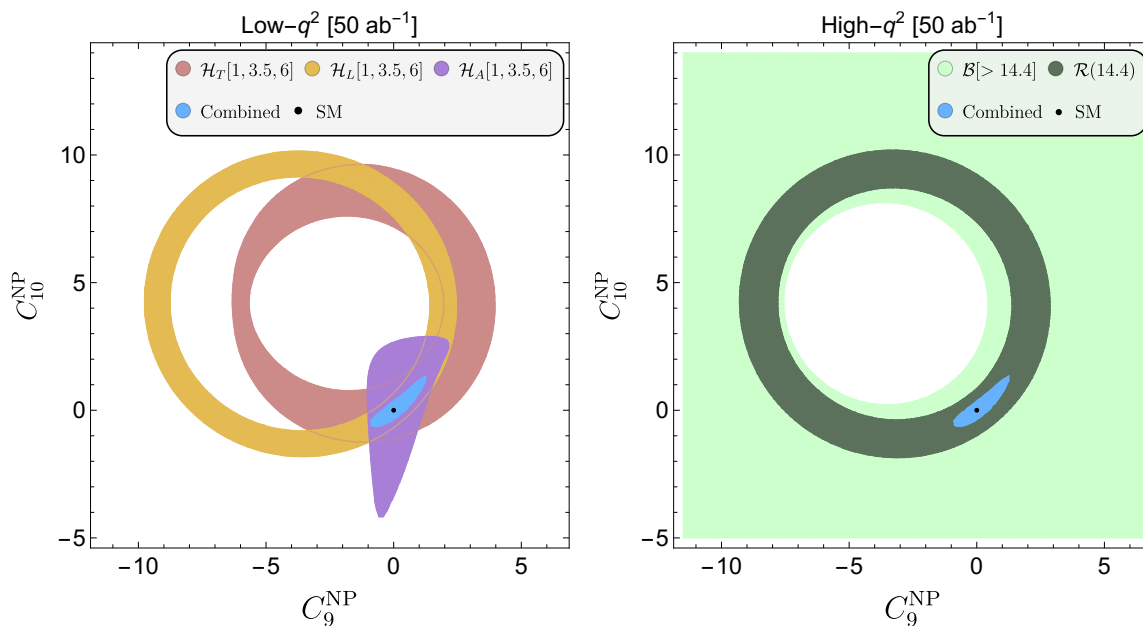
Figure 4. Breakdown of the projected constraints at low- and high-q^2. See the caption in figure 2 for further details.
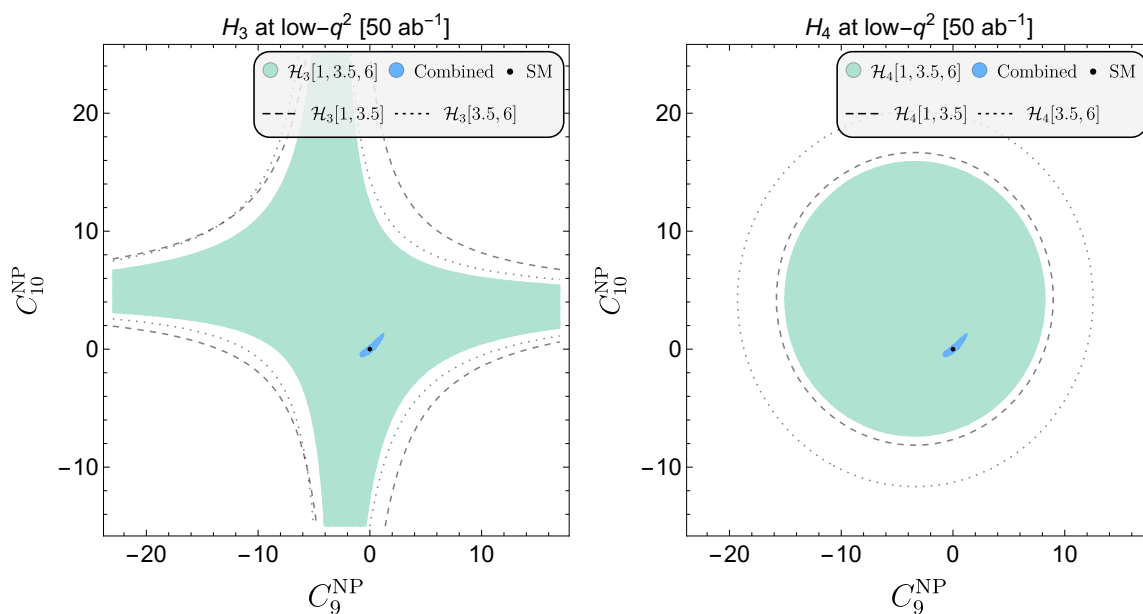
Figure 5. Projected constraints from the QED observables $\mathcal{H}_3$ and $\mathcal{H}_4$ at low-q^2. See the caption in figure 2 for further details.
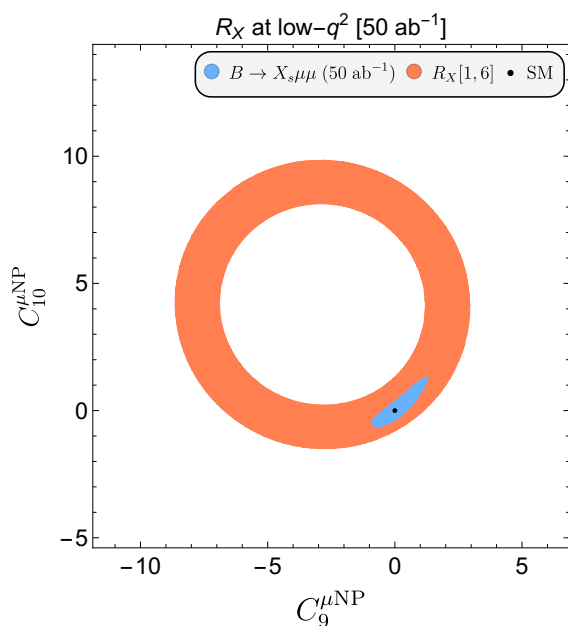
Figure 6. The expected 50 ab^{-1} bounds under the assumption $C^e_{9,10} = C^{e\text{SM}}_{9,10}$. The combined contour is slightly larger than the one in figure 2 because it corresponds to the muon channel only.
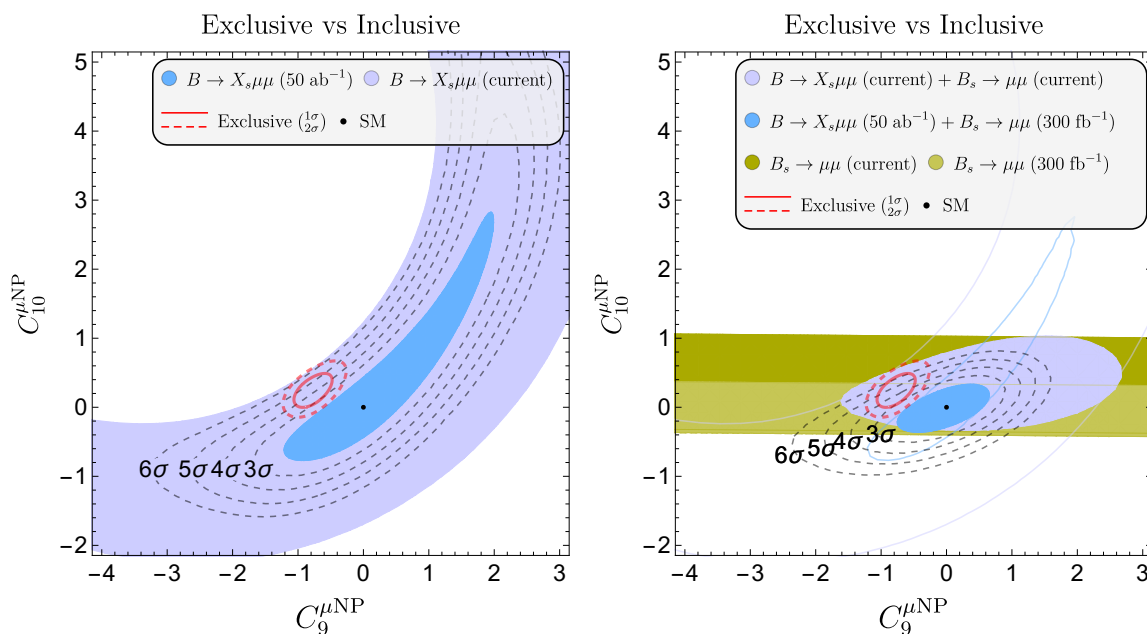
Figure 7. Comparison between the expected bounds from inclusive measurements (up to six standard deviations) with the bounds from existing exclusive $b \to s\ell^+\ell^-$ measurements. The latter are derived using the Flavio [80] and Smelli [81] packages and include constraints from branching ratio and asymmetries in $b \to s\mu^+\mu^-$ as well as from the lepton flavour universality violating ratios $R_{K^{(*)}}$. In the right panel we combine inclusive $\bar{B} \to X_s\mu^+\mu^-$ with the current determination of $\mathcal{B}(\bar{B}_s \to \mu^+\mu^-)$.

We begin by recalculating the expected constraints for the $\bar{B} \to X_s \mu^+ \mu^-$ channel only (i.e. the projected statistical experimental uncertainties increase by $\sqrt{2}$ because we loose the di-electron final state). The resulting projected Belle II reach is displayed in figure 6, where we also include the expected constraints from measurements of the ratio R_{X_s} (which is essentially free of theoretical uncertainties, see the SM predictions given in section 3.3). The constraints from R_{X_s} are weaker than those from $\mathcal{H}_{T,L}$ mainly because of the much larger experimental statistical uncertainty: the ratio of the di-muon rate to the di-electron one has an expected statistical uncertainty which is twice as large than that for the combined electron and muon channel. Nevertheless, the absence of theoretical uncertainties makes this observable very interesting.

In the left panel of figure 7 we compare the expected constraints from inclusive di-muon modes with the existing bounds from exclusive $b \to s\mu^+\mu^-$ observables. The exclusive contour has been calculated with the packages Flavio [80] and Smelli [81] using the default likelihood but without the inclusion of $\bar{B}_s \to \mu^+\mu^-$. We see that if $C_{9,10}^{\mu\mathrm{NP}} = 0$, Belle II results of the inclusive observables will exclude the current best-fit point of the exclusive fits by slightly more than 4σ. Moreover, we checked in a separate study that if the true values of $C_{9,10}^{\mu\mathrm{NP}}$ are at the current best fit point of the fit to the exclusive data, the SM point would be excluded with a similar significance.

In the right panel of figure 7 we show the impact of $B_s \to \mu^+\mu^-$, which is essentially only dependent on the coefficient C_{10}^μ. We choose to include the constraint from this purely leptonic decay in the inclusive semileptonic expected reach because both modes are considerably cleaner than the various exclusive semileptonic observables. The currently allowed region is obtained by including the PDG average $\mathcal{B}(B_s \to \mu^+\mu^-) = (3.0 \pm 0.4) \times 10^{-9}$ and the theoretical description outlined in ref. [82]. The projected contour is obtained by assuming a $B_s \to \mu^+\mu^-$ measurement centered on the SM expectation [82] with an uncertainty corresponding to $300\,\mathrm{fb}^{-1}$ of LHCb data (which is the High-Luminosity LHC scenario considered in ref. [83]). After including $B_s \to \mu^+\mu^-$, the reach in the $[C_9^{\mu\mathrm{NP}}, C_{10}^{\mu\mathrm{NP}}]$ plane improves even further and the current exclusive best-fit point could be excluded with a significance close to 5σ if $C_{9,10}^{\mu\mathrm{NP}} = 0$.

5.2 Interplay with $b \to s\tau^+\tau^-$

The $b \to s\tau^+\tau^-$ decays, both the exclusive and inclusive modes, are very challenging to measure in experiments. The current experimental bounds on the decay rates are still far away from the corresponding SM expectations [84, 85]. Alternatively, the $\tau^+\tau^-$ final state can be indirectly constrained by using the exclusive decay $B^+ \to K^+\mu^+\mu^-$, which receives contributions from the $\tau^+\tau^-$ state via re-scattering [86].

Similar re-scattering also occurs in the inclusive channel, therefore $\bar{B} \to X_s \ell^+\ell^-$ measurements can be used to constrain the $b \to s\tau^+\tau^-$ amplitude. Defining, $C_9^\tau(\mu_0) \equiv$

$R_9^\tau C_9^{\rm SM}(\mu_0)$, we find

$$\mathcal{B}[1,6] = \mathcal{B}_{\rm SM}[1,6] - \left[2.9 \times 10^{-3}\,\mathcal{R}\left(R_9^\tau - 1\right) + 4.8 \times 10^{-5}\,\mathcal{I}\left(R_9^\tau\right)\right] \times 10^{-7}\,,$$
$$\mathcal{B}[1,3.5] = \mathcal{B}_{\rm SM}[1,3.5] - \left[8.5 \times 10^{-4}\,\mathcal{R}\left(R_9^\tau - 1\right) + 1.8 \times 10^{-5}\,\mathcal{I}\left(R_9^\tau\right)\right] \times 10^{-7}\,,$$
$$\mathcal{B}[3.5,6] = \mathcal{B}_{\rm SM}[3.5,6] - \left[2.1 \times 10^{-3}\,\mathcal{R}\left(R_9^\tau - 1\right) + 2.9 \times 10^{-5}\,\mathcal{I}\left(R_9^\tau\right)\right] \times 10^{-7}\,,$$
$$\mathcal{B}[> 14.4] = \mathcal{B}_{\rm SM}[> 14.4] + \left[3.8 \times 10^{-3}\,\mathcal{R}\left(R_9^\tau - 1\right) - 3.6 \times 10^{-3}\,\mathcal{I}\left(R_9^\tau\right)\right] \times 10^{-7}\,. \quad (5.4)$$

We observe that the high-q^2 branching ratio $\mathcal{B}[> 14.4]$ is most sensitive to C_9^τ. For the sake of simplicity we assume that C_9^τ is real. Assuming a projected uncertainty of 4.7% on $\mathcal{B}[> 14.4]$ at Belle II (see table 4) [21] leads to

$$R_9^\tau \approx 0 \pm 230\,, \qquad \mathcal{B}(B^+ \to K^+\tau^+\tau^-) \lesssim \left\{ \begin{array}{ll} 2.5 \times 10^{-3}\,, & \text{if } C_{10}^\tau = 0\,, \\ 8.1 \times 10^{-3}\,, & \text{if } C_{10}^\tau = C_9^\tau\,. \end{array} \right. \quad (5.5)$$

This result is competitive to the current direct bound given by BaBar, $\mathcal{B}(B^+ \to K^+\tau^+\tau^-) < 2.25 \times 10^{-3}$ at 90% CL [84]. Similar sensitivity can be obtained by considering $\mathcal{R}(14.4)$ which has a slightly larger projected experimental uncertainty $[\delta\mathcal{R}(14.4)]^{\rm exp}_{50\,{\rm ab}^{-1}} = 7.3\%$ (as discussed in the previous section) but a much smaller theoretical uncertainty than $\mathcal{B}[> 14.4]$. We find

$$R_9^\tau \approx 0 \pm 66\,, \qquad \mathcal{B}(B^+ \to K^+\tau^+\tau^-) \lesssim \left\{ \begin{array}{ll} 2.1 \times 10^{-4}\,, & \text{if } C_{10}^\tau = 0\,, \\ 6.7 \times 10^{-4}\,, & \text{if } C_{10}^\tau = C_9^\tau\,. \end{array} \right. \quad (5.6)$$

This indirect constraint from the Belle II measurement of $\bar{B} \to X_s\mu^+\mu^-$ is comparable with the direct $B^+ \to K^+\tau^+\tau^-$ measurement with the LHCb upgrade-II luminosity [86].

6 Conclusion

In the absence of direct signals for physics beyond the SM, FCNC decays play a crucial role in searching for imprints of new physics in low-energy processes. With the experimental programs at LHCb, Belle II and other experiments in operation, we are entering a new era of precision measurements of rare B decays. One of the prime measurements which is expected to become available for the first time at Belle II is a full angular analysis of inclusive $\bar{B} \to X_s\ell^+\ell^-$. This analysis is interesting on its own grounds, but also offers a unique opportunity to study the interplay with its exclusive $b \to s\ell^+\ell^-$ counterparts. In order to pave to road for precision phenomenology and extensive new-physics studies, a theoretical update of inclusive $\bar{B} \to X_s\ell^+\ell^-$ is mandatory.

In this paper we therefore presented a comprehensive update of the SM theory predictions for the entire set of inclusive $\bar{B} \to X_s\ell^+\ell^-$ observables. As new observables we present predictions for the ratio R_{X_s} (and similarly for the angular parts). These are ratios of the inclusive $\bar{B} \to X_s\mu^+\mu^-$ versus $\bar{B} \to X_s e^+e^-$ transitions sensitive to lepton-flavour universality, in analogy to the exclusive ratios $R_{K^{(*)}}$. Other main novelties in our analysis are updated input parameters, the implementation of the new and more sophisticated

treatment of non-perturbative effects via the Krüger-Sehgal mechanism [50], and the inclusion of non-local power corrections via the resolved contributions [51–53]. Along the lines of [50] we also implement the results of the updated study of power-suppressed effects in the high-q^2 region. Depending on the observable and the q^2-range, this leads to central values which differ by several percent from those in our previous analysis [40]. For example, the low-q^2 integrated branching ratio for muons in units of 10^{-6} moves from 1.62 ± 0.09 to 1.73 ± 0.13, where the increase in uncertainty can be almost entirely attributed to the additional 5% that we add to take into account the resolved contributions.

In addition, we investigated the effect of collinear photons in a detailed Monte Carlo study and gave a prescription for how to deal with these effects at Belle II. An effect which has not been included in previous analysis is the bin migration from the charmonium resonances into the perturbative low-q^2 window. Table 3 contains a complete list of correction factors that have to be applied to compare our predictions for the electron channel (in which we always adopt the defintion $q^2 = (p_{e^+} + p_{e^-})^2$) to the Belle II analysis which applies angular and energy cuts on collinear photons.

Finally, we presented an elaborate discussion on the new physics potential of inclusive $\bar{B} \to X_s \ell^+ \ell^-$. First, we studied the bounds from current measurements, which are still rather loose. However, the projection to the final Belle II data set and the inclusion of all angular observables reveal that the inclusive channel has already power enough on its own to tightly constrain C_9^{NP} and C_{10}^{NP}. In combination with exclusive $b \to s\ell^+ \ell^-$ decays and the rare $\bar{B}_s \to \mu^+ \mu^-$ decay, the full power of the synergy between inclusive and exclusive FCNC transitions becomes manifest. Should the true value of C_9^{NP} and C_{10}^{NP} be at either the SM point $C_9^{\mathrm{NP}} = C_{10}^{\mathrm{NP}} = 0$ or the current best-fit point of the exclusive fits, an analysis of inclusive $\bar{B} \to X_s \ell^+ \ell^-$ at Belle II with 50ab^{-1} of data will prefer that one with respect to the other one at the level of $\sim 5\sigma$. This again underlines the necessity of a full angular analysis of $\bar{B} \to X_s \ell^+ \ell^-$ at Belle II.

A point we addressed only marginally in the present article is that of a cut on the hadronic invariant mass M_X. While there is hope that a fully inclusive measurement using the recoil technique will become feasible towards the end of Belle II, such a cut will remain necessary for a good portion of the Belle II operation time. Despite the fact that there exists preliminary work on this topic [57–59], better knowledge of sub-leading shape functions will certainly be required for more precise predictions. As for now, only the zero crossing of the forward backward asymmetry has been calculated in the presence of an M_X cut [60]. A study on the effect of a hadronic mass cut on the other observables will also build on [51–53] and is left for future work.

Acknowledgments

q^2 range [GeV^2]	$[1,6]$	$[1,3.5]$	$[3.5,6]$
$\mathcal{B}$	16.98×10^{-7}	9.23×10^{-7}	7.75×10^{-7}
$\mathcal{H}_T$	3.13×10^{-7}	1.48×10^{-7}	1.64×10^{-7}
$\mathcal{H}_L$	13.77×10^{-7}	7.69×10^{-7}	6.08×10^{-7}
$\mathcal{H}_A$	-0.27×10^{-7}	-1.08×10^{-7}	0.81×10^{-7}
q^2 range [GeV^2]	> 14.4		
$\mathcal{B}$	2.59×10^{-7}		
$\mathcal{R}(s_0)$	27.71×10^{-4}		

Table 5. Phenomenological results without electromagnetic effects, i.e. log-enhanced QED corrections to the matrix elements at the scale μ_b are not included. The smaller effect of QED corrections in the matching and running is, however, taken into accout.

A   Phenomenological results

In this appendix, we give the numerical results for the low-q^2 observables $\mathcal{H}_A, \mathcal{H}_T, \mathcal{H}_L, \mathcal{H}_3$ and $\mathcal{H}_4$ which we relegated from section 3. In table 5, we list all observables without electromagnetic effects to also account for the case that electromagnetic radiation is taken care of entirely on the experimental side.

A.1 $\mathcal{H}_A$

$$\mathcal{H}_A[1,3.5]_{ee} = (-0.95 \pm 0.05_{\text{scale}} \pm 0.008_{m_t} \pm 0.006_{C,m_c} \pm 0.02_{m_b} \pm 0.02_{\alpha_s} \pm 0.001_{\text{CKM}}$$
$$\pm 0.01_{\text{BR}_{\text{sl}}} \pm 0.0002_{\lambda_2} \pm 0.05_{\text{resolved}}) \cdot 10^{-7} = (-0.95 \pm 0.08) \cdot 10^{-7},$$

$$\mathcal{H}_A[3.5,6]_{ee} = (0.91 \pm 0.13_{\text{scale}} \pm 0.009_{m_t} \pm 0.04_{C,m_c} \pm 0.05_{m_b} \pm 0.03_{\alpha_s} \pm 0.001_{\text{CKM}}$$
$$\pm 0.01_{\text{BR}_{\text{sl}}} \pm 0.005_{\lambda_2} \pm 0.05_{\text{resolved}}) \cdot 10^{-7} = (0.91 \pm 0.16) \cdot 10^{-7},$$

$$\mathcal{H}_A[1,6]_{ee} = (-0.04 \pm 0.19_{\text{scale}} \pm 0.0004_{m_t} \pm 0.03_{C,m_c} \pm 0.07_{m_b} \pm 0.05_{\alpha_s} \pm 0.00004_{\text{CKM}}$$
$$\pm 0.0006_{\text{BR}_{\text{sl}}} \pm 0.005_{\lambda_2} \pm 0.002_{\text{resolved}}) \cdot 10^{-7} = (-0.04 \pm 0.21) \cdot 10^{-7}. \quad \text{(A.1)}$$

$$\mathcal{H}_A[1,3.5]_{\mu\mu} = (-1.03 \pm 0.05_{\text{scale}} \pm 0.009_{m_t} \pm 0.007_{C,m_c} \pm 0.02_{m_b} \pm 0.02_{\alpha_s} \pm 0.0009_{\text{CKM}}$$
$$\pm 0.02_{\text{BR}_{\text{sl}}} \pm 0.0006_{\lambda_2} \pm 0.05_{\text{resolved}}) \cdot 10^{-7} = (-1.03 \pm 0.08) \cdot 10^{-7},$$

$$\mathcal{H}_{\mathrm{A}}[3.5,6]_{\mu\mu} = (0.85 \pm 0.13_{\mathrm{scale}} \pm 0.008_{m_t} \pm 0.03_{C,m_c} \pm 0.05_{m_b} \pm 0.03_{\alpha_s} \pm 0.0008_{\mathrm{CKM}}$$
$$\pm 0.01_{\mathrm{BR_{sl}}} \pm 0.005_{\lambda_2} \pm 0.04_{\mathrm{resolved}}) \cdot 10^{-7} = (0.85 \pm 0.16) \cdot 10^{-7},$$
$$\mathcal{H}_{\mathrm{A}}[1,6]_{\mu\mu} = (-0.18 \pm 0.19_{\mathrm{scale}} \pm 0.0009_{m_t} \pm 0.03_{C,m_c} \pm 0.07_{m_b} \pm 0.05_{\alpha_s} \pm 0.0002_{\mathrm{CKM}}$$
$$\pm 0.003_{\mathrm{BR_{sl}}} \pm 0.006_{\lambda_2} \pm 0.009_{\mathrm{resolved}}) \cdot 10^{-7} = (-0.18 \pm 0.21) \cdot 10^{-7}. \quad (A.2)$$

A.2 $\mathcal{H}_T$ and $\mathcal{H}_L$

$$\mathcal{H}_T[1,3.5]_{ee} = (2.91 \pm 0.15_{\mathrm{scale}} \pm 0.03_{m_t} \pm 0.05_{C,m_c} \pm 0.02_{m_b} \pm 0.005_{\alpha_s} \pm 0.003_{\mathrm{CKM}}$$
$$\pm 0.04_{\mathrm{BR_{sl}}} \pm 0.01_{\lambda_1} \pm 0.004_{\lambda_2} \pm 0.15_{\mathrm{resolved}}) \cdot 10^{-7} = (2.91 \pm 0.22) \cdot 10^{-7},$$
$$\mathcal{H}_T[3.5,6]_{ee} = (2.51 \pm 0.18\mathrm{scale} \pm 0.03_{m_t} \pm 0.06_{C,m_c} \pm 0.05_{m_b} \pm 0.02_{\alpha_s} \pm 0.002_{\mathrm{CKM}}$$
$$\pm 0.04_{\mathrm{BR_{sl}}} \pm 0.02_{\lambda_1} \pm 0.003_{\lambda_2} \pm 0.13_{\mathrm{resolved}}) \cdot 10^{-7} = (2.51 \pm 0.24) \cdot 10^{-7},$$
$$\mathcal{H}_T[1,6]_{ee} = (5.42 \pm 0.33_{\mathrm{scale}} \pm 0.07_{m_t} \pm 0.11_{C,m_c} \pm 0.07_{m_b} \pm 0.01_{\alpha_s} \pm 0.005_{\mathrm{CKM}}$$
$$\pm 0.08_{\mathrm{BR_{sl}}} \pm 0.04_{\lambda_1} \pm 0.007_{\lambda_2} \pm 0.27_{\mathrm{resolved}}) \cdot 10^{-7} = (5.42 \pm 0.46) \cdot 10^{-7}. \quad (A.3)$$
$$\mathcal{H}_T[1,3.5]_{\mu\mu} = (2.08 \pm 0.08_{\mathrm{scale}} \pm 0.02_{m_t} \pm 0.03_{C,m_c} \pm 0.01_{m_b} \pm 0.009_{\alpha_s} \pm 0.002_{\mathrm{CKM}}$$
$$\pm 0.03_{\mathrm{BR_{sl}}} \pm 0.01_{\lambda_1} \pm 0.0005_{\lambda_2} \pm 0.10_{\mathrm{resolved}}) \cdot 10^{-7} = (2.08 \pm 0.14) \cdot 10^{-7},$$
$$\mathcal{H}_T[3.5,6]_{\mu\mu} = (2.00 \pm 0.15_{\mathrm{scale}} \pm 0.03_{m_t} \pm 0.05_{C,m_c} \pm 0.05_{m_b} \pm 0.01_{\alpha_s} \pm 0.002_{\mathrm{CKM}}$$
$$\pm 0.03_{\mathrm{BR_{sl}}} \pm 0.02_{\lambda_1} \pm 0.0007_{\lambda_2} \pm 0.10_{\mathrm{resolved}}) \cdot 10^{-7} = (2.00 \pm 0.20) \cdot 10^{-7},$$
$$\mathcal{H}_T[1,6]_{\mu\mu} = (4.08 \pm 0.23_{\mathrm{scale}} \pm 0.05_{m_t} \pm 0.08_{C,m_c} \pm 0.06_{m_b} \pm 0.005_{\alpha_s} \pm 0.004_{\mathrm{CKM}}$$
$$\pm 0.06_{\mathrm{BR_{sl}}} \pm 0.03_{\lambda_1} \pm 0.001_{\lambda_2} \pm 0.20_{\mathrm{resolved}}) \cdot 10^{-7} = (4.08 \pm 0.34) \cdot 10^{-7}. \quad (A.4)$$
$$\mathcal{H}_L[1,3.5]_{ee} = (6.92 \pm 0.28_{\mathrm{scale}} \pm 0.07_{m_t} \pm 0.16_{C,m_c} \pm 0.09_{m_b} \pm 0.05_{\alpha_s} \pm 0.006_{\mathrm{CKM}}$$
$$\pm 0.10_{\mathrm{BR_{sl}}} \pm 0.01_{\lambda_1} \pm 0.06_{\lambda_2} \pm 0.35_{\mathrm{resolved}}) \cdot 10^{-7} = (6.92 \pm 0.50) \cdot 10^{-7},$$
$$\mathcal{H}_L[3.5,6]_{ee} = (5.43 \pm 0.29_{\mathrm{scale}} \pm 0.06_{m_t} \pm 0.13_{C,m_c} \pm 0.04_{m_b} \pm 0.04_{\alpha_s} \pm 0.005_{\mathrm{CKM}}$$
$$\pm 0.08_{\mathrm{BR_{sl}}} \pm 0.02_{\lambda_1} \pm 0.05_{\lambda_2} \pm 0.27_{\mathrm{resolved}}) \cdot 10^{-7} = (5.43 \pm 0.44) \cdot 10^{-7},$$
$$\mathcal{H}_L[1,6]_{ee} = (12.35 \pm 0.53_{\mathrm{scale}} \pm 0.13_{m_t} \pm 0.29_{C,m_c} \pm 0.14_{m_b} \pm 0.09_{\alpha_s} \pm 0.01_{\mathrm{CKM}}$$
$$\pm 0.19_{\mathrm{BR_{sl}}} \pm 0.03_{\lambda_1} \pm 0.11_{\lambda_2} \pm 0.62_{\mathrm{resolved}}) \cdot 10^{-7} = (12.35 \pm 0.92) \cdot 10^{-7}. \quad (A.5)$$
$$\mathcal{H}_L[1,3.5]_{\mu\mu} = (7.37 \pm 0.28_{\mathrm{scale}} \pm 0.08_{m_t} \pm 0.17_{C,m_c} \pm 0.10_{m_b} \pm 0.05_{\alpha_s} \pm 0.007_{\mathrm{CKM}}$$
$$\pm 0.11_{\mathrm{BR_{sl}}} \pm 0.01_{\lambda_1} \pm 0.06_{\lambda_2} \pm 0.37_{\mathrm{resolved}}) \cdot 10^{-7} = (7.37 \pm 0.52) \cdot 10^{-7},$$
$$\mathcal{H}_L[3.5,6]_{\mu\mu} = (5.81 \pm 0.31_{\mathrm{scale}} \pm 0.06_{m_t} \pm 0.14_{C,m_c} \pm 0.05_{m_b} \pm 0.04_{\alpha_s} \pm 0.005_{\mathrm{CKM}}$$
$$\pm 0.09_{\mathrm{BR_{sl}}} \pm 0.02_{\lambda_1} \pm 0.06_{\lambda_2} \pm 0.29_{\mathrm{resolved}}) \cdot 10^{-7} = (5.81 \pm 0.47) \cdot 10^{-7},$$
$$\mathcal{H}_L[1,6]_{\mu\mu} = (13.18 \pm 0.53_{\mathrm{scale}} \pm 0.14_{m_t} \pm 0.31_{C,m_c} \pm 0.15_{m_b} \pm 0.09_{\alpha_s} \pm 0.01_{\mathrm{CKM}}$$
$$\pm 0.20_{\mathrm{BR_{sl}}} \pm 0.03_{\lambda_1} \pm 0.12_{\lambda_2} \pm 0.66_{\mathrm{resolved}}) \cdot 10^{-7} = (13.18 \pm 0.96) \cdot 10^{-7}. \quad (A.6)$$

A.3 $\mathcal{H}_3$ and $\mathcal{H}_4$

$$\mathcal{H}_3[1,3.5]_{ee} = (4.14 \pm 0.65_{\mathrm{scale}} \pm 0.04_{m_t} \pm 0.09_{C,m_c} \pm 0.10_{m_b} \pm 0.05_{\alpha_s} \pm 0.004_{\mathrm{CKM}}$$
$$\pm 0.06_{\mathrm{BR_{sl}}} \pm 0.01_{\lambda_1} \pm 0.02_{\lambda_2} \pm 0.21_{\mathrm{resolved}}) \cdot 10^{-9} = (4.14 \pm 0.70) \cdot 10^{-9},$$
$$\mathcal{H}_3[3.5,6]_{ee} = (5.00 \pm 0.51_{\mathrm{scale}} \pm 0.05_{m_t} \pm 0.11_{C,m_c} \pm 0.07_{m_b} \pm 0.04_{\alpha_s} \pm 0.005_{\mathrm{CKM}}$$
$$\pm 0.08_{\mathrm{BR_{sl}}} \pm 0.01_{\lambda_1} \pm 0.02_{\lambda_2} \pm 0.25_{\mathrm{resolved}}) \cdot 10^{-9} = (5.00 \pm 0.59) \cdot 10^{-9},$$

$$\mathcal{H}_3[1,6]_{ee} = (9.14 \pm 1.16_{\text{scale}} \pm 0.09_{m_t} \pm 0.19_{C,m_c} \pm 0.17_{m_b} \pm 0.09_{\alpha_s} \pm 0.008_{\text{CKM}}$$
$$\pm 0.14_{\text{BR}_{\text{sl}}} \pm 0.02_{\lambda_1} \pm 0.04_{\lambda_2} \pm 0.46_{\text{resolved}}) \cdot 10^{-9} = (9.14 \pm 1.29) \cdot 10^{-9}. \quad \text{(A.7)}$$

$$\mathcal{H}_3[1,3.5]_{\mu\mu} = (1.72 \pm 0.27_{\text{scale}} \pm 0.02_{m_t} \pm 0.04_{C,m_c} \pm 0.04_{m_b} \pm 0.02_{\alpha_s} \pm 0.002_{\text{CKM}}$$
$$\pm 0.03_{\text{BR}_{\text{sl}}} \pm 0.004_{\lambda_1} \pm 0.01_{\lambda_2} \pm 0.09_{\text{resolved}}) \cdot 10^{-9} = (1.72 \pm 0.29) \cdot 10^{-9},$$

$$\mathcal{H}_3[3.5,6]_{\mu\mu} = (2.08 \pm 0.21_{\text{scale}} \pm 0.02_{m_t} \pm 0.04_{C,m_c} \pm 0.03_{m_b} \pm 0.02_{\alpha_s} \pm 0.002_{\text{CKM}}$$
$$\pm 0.03_{\text{BR}_{\text{sl}}} \pm 0.005_{\lambda_1} \pm 0.01_{\lambda_2} \pm 0.10_{\text{resolved}}) \cdot 10^{-9} = (2.08 \pm 0.25) \cdot 10^{-9},$$

$$\mathcal{H}_3[1,6]_{\mu\mu} = (3.80 \pm 0.48_{\text{scale}} \pm 0.04_{m_t} \pm 0.08_{C,m_c} \pm 0.06_{m_b} \pm 0.04_{\alpha_s} \pm 0.003_{\text{CKM}}$$
$$\pm 0.06_{\text{BR}_{\text{sl}}} \pm 0.01_{\lambda_1} \pm 0.02_{\lambda_2} \pm 0.19_{\text{resolved}}) \cdot 10^{-9} = (3.80 \pm 0.53) \cdot 10^{-9}. \quad \text{(A.8)}$$

$$\mathcal{H}_4[1,3.5]_{ee} = (6.37 \pm 0.56_{\text{scale}} \pm 0.07_{m_t} \pm 0.13_{C,m_c} \pm 0.01_{m_b} \pm 0.03_{\alpha_s} \pm 0.006_{\text{CKM}}$$
$$\pm 0.10_{\text{BR}_{\text{sl}}} \pm 0.01_{\lambda_1} \pm 0.03_{\lambda_2} \pm 0.32_{\text{resolved}}) \cdot 10^{-9} = (6.37 \pm 0.67) \cdot 10^{-9},$$

$$\mathcal{H}_4[3.5,6]_{ee} = (2.24 \pm 0.16_{\text{scale}} \pm 0.03_{m_t} \pm 0.05_{C,m_c} \pm 0.02_{m_b} \pm 0.01_{\alpha_s} \pm 0.002_{\text{CKM}}$$
$$\pm 0.03_{\text{BR}_{\text{sl}}} \pm 0.005_{\lambda_1} \pm 0.01_{\lambda_2} \pm 0.11_{\text{resolved}}) \cdot 10^{-9} = (2.24 \pm 0.21) \cdot 10^{-9},$$

$$\mathcal{H}_4[1,6]_{ee} = (8.60 \pm 0.73_{\text{scale}} \pm 0.09_{m_t} \pm 0.18_{C,m_c} \pm 0.02_{m_b} \pm 0.04_{\alpha_s} \pm 0.008_{\text{CKM}}$$
$$\pm 0.13_{\text{BR}_{\text{sl}}} \pm 0.02_{\lambda_1} \pm 0.04_{\lambda_2} \pm 0.43_{\text{resolved}}) \cdot 10^{-9} = (8.60 \pm 0.88) \cdot 10^{-9}. \quad \text{(A.9)}$$

$$\mathcal{H}_4[1,3.5]_{\mu\mu} = (2.65 \pm 0.23_{\text{scale}} \pm 0.03_{m_t} \pm 0.06_{C,m_c} \pm 0.01_{m_b} \pm 0.01_{\alpha_s} \pm 0.002_{\text{CKM}}$$
$$\pm 0.04_{\text{BR}_{\text{sl}}} \pm 0.01_{\lambda_1} \pm 0.01_{\lambda_2} \pm 0.13_{\text{resolved}}) \cdot 10^{-9} = (2.65 \pm 0.28) \cdot 10^{-9},$$

$$\mathcal{H}_4[3.5,6]_{\mu\mu} = (0.93 \pm 0.07_{\text{scale}} \pm 0.01_{m_t} \pm 0.02_{C,m_c} \pm 0.01_{m_b} \pm 0.004_{\alpha_s} \pm 0.001_{\text{CKM}}$$
$$\pm 0.01_{\text{BR}_{\text{sl}}} \pm 0.002_{\lambda_1} \pm 0.005_{\lambda_2} \pm 0.05_{\text{resolved}}) \cdot 10^{-9} = (0.93 \pm 0.09) \cdot 10^{-9},$$

$$\mathcal{H}_4[1,6]_{\mu\mu} = (3.58 \pm 0.30_{\text{scale}} \pm 0.04_{m_t} \pm 0.08_{C,m_c} \pm 0.02_{m_b} \pm 0.02_{\alpha_s} \pm 0.003_{\text{CKM}}$$
$$\pm 0.05_{\text{BR}_{\text{sl}}} \pm 0.01_{\lambda_1} \pm 0.02_{\lambda_2} \pm 0.18_{\text{resolved}}) \cdot 10^{-9} = (3.58 \pm 0.36) \cdot 10^{-9}. \quad \text{(A.10)}$$

B   New physics formulas

In this appendix we give the new-physics formulas of all observables in terms of the following ratios

$$R_{7,8} = \frac{C_{7,8}^{(00)\text{eff}}(\mu_0)}{C_{7,8}^{(00)\text{eff,SM}}(\mu_0)} \qquad \text{and} \qquad R_{9,10} = \frac{C_{9,10}^{(11)}(\mu_0)}{C_{9,10}^{(11)\text{SM}}(\mu_0)} \,. \quad \text{(B.1)}$$

The superscripts on the Wilson coefficients denote the order in the expansion in α_s and $\kappa = \alpha_e/\alpha_s$, see [38, 40] for details. The connection to the new-physics part of the Wilson coefficients in eq. (5.1) is straightforward. On the right-hand sides of all the equations below, $\mathcal{R}$ and $\mathcal{I}$ denote the real and imaginary part of the expression in parenthesis, respectively. The label 'no em' refers to leaving out log-enhanced QED corrections as described in the caption of table 5. The new-physics formulas are provided electronically as supplementary material attached to the submission of the present paper.

B.1   Branching ratio, low-q^2 region

$$\mathcal{B}[1,3.5]_{ee} = \Big[0.216997 \, |R_7|^2 + 0.00294962 \, |R_8|^2 + 0.833492 \, |R_9|^2$$
$$+ 6.0782 \, |R_{10}|^2 + 0.0173276 \mathcal{I}(R_7 R_8^*) + 0.00288963 \mathcal{I}(R_7 R_9^*)$$

$$
\begin{aligned}
&+ 0.0151859\,\mathcal{I}\left(R_8 R_9^*\right) - 0.000309907\,\mathcal{I}\left(R_8 R_{10}^*\right) + 0.0519547\,\mathcal{R}\left(R_7 R_8^*\right) \\
&- 0.519361\,\mathcal{R}\left(R_7 R_9^*\right) + 0.00893145\,\mathcal{R}\left(R_7 R_{10}^*\right) - 0.0597428\,\mathcal{R}\left(R_8 R_9^*\right) \\
&+ 0.00109835\,\mathcal{R}\left(R_8 R_{10}^*\right) - 0.0573964\,\mathcal{R}\left(R_9 R_{10}^*\right) + 0.0183294\,\mathcal{I}\left(R_7\right) \\
&- 0.00310346\,\mathcal{I}\left(R_8\right) + 0.0477963\,\mathcal{I}\left(R_9\right) - 0.0020085\,\mathcal{I}\left(R_{10}\right) \\
&+ 0.12521\,\mathcal{R}\left(R_7\right) + 0.00686405\,\mathcal{R}\left(R_8\right) + 1.66745\,\mathcal{R}\left(R_9\right) \\
&- 0.296469\,\mathcal{R}\left(R_{10}\right) + 1.76389 \Big] \times 10^{-7}, \quad\quad\quad\quad\quad\quad\quad\text{(B.2)}
\end{aligned}
$$

$$
\begin{aligned}
\mathcal{B}[3.5,6]_{ee} =\ & \Big[0.0713305\,|R_7|^2 + 0.000898232\,|R_8|^2 + 0.731636\,|R_9|^2 \\
&+ 5.28065\,|R_{10}|^2 + 0.00587951\,\mathcal{I}\left(R_7 R_8^*\right) + 0.0021872\,\mathcal{I}\left(R_7 R_9^*\right) \\
&+ 0.0114944\,\mathcal{I}\left(R_8 R_9^*\right) - 0.000234573\,\mathcal{I}\left(R_8 R_{10}^*\right) + 0.0170293\,\mathcal{R}\left(R_7 R_8^*\right) \\
&- 0.370929\,\mathcal{R}\left(R_7 R_9^*\right) + 0.00675653\,\mathcal{R}\left(R_7 R_{10}^*\right) - 0.0415991\,\mathcal{R}\left(R_8 R_9^*\right) \\
&+ 0.000790901\,\mathcal{R}\left(R_8 R_{10}^*\right) - 0.0524327\,\mathcal{R}\left(R_9 R_{10}^*\right) + 0.0120584\,\mathcal{I}\left(R_7\right) \\
&+ 0.00940699\,\mathcal{I}\left(R_8\right) + 0.000191673\,\mathcal{I}\left(R_9\right) - 0.000977984\,\mathcal{I}\left(R_{10}\right) \\
&- 0.370247\,\mathcal{R}\left(R_7\right) - 0.0404915\,\mathcal{R}\left(R_8\right) + 1.77487\,\mathcal{R}\left(R_9\right) \\
&- 0.274818\,\mathcal{R}\left(R_{10}\right) + 1.2456 \Big] \times 10^{-7}, \quad\quad\quad\quad\quad\quad\quad\text{(B.3)}
\end{aligned}
$$

$$
\begin{aligned}
\mathcal{B}[1,6]_{ee} =\ & \Big[0.288327\,|R_7|^2 + 0.00384785\,|R_8|^2 + 1.56513\,|R_9|^2 \\
&+ 11.3588\,|R_{10}|^2 + 0.0232071\,\mathcal{I}\left(R_7 R_8^*\right) + 0.00507683\,\mathcal{I}\left(R_7 R_9^*\right) \\
&+ 0.0266804\,\mathcal{I}\left(R_8 R_9^*\right) - 0.00054448\,\mathcal{I}\left(R_8 R_{10}^*\right) + 0.068984\,\mathcal{R}\left(R_7 R_8^*\right) \\
&- 0.89029\,\mathcal{R}\left(R_7 R_9^*\right) + 0.015688\,\mathcal{R}\left(R_7 R_{10}^*\right) - 0.101342\,\mathcal{R}\left(R_8 R_9^*\right) \\
&+ 0.00188925\,\mathcal{R}\left(R_8 R_{10}^*\right) - 0.109829\,\mathcal{R}\left(R_9 R_{10}^*\right) + 0.0303878\,\mathcal{I}\left(R_7\right) \\
&+ 0.00630353\,\mathcal{I}\left(R_8\right) + 0.047988\,\mathcal{I}\left(R_9\right) - 0.00298649\,\mathcal{I}\left(R_{10}\right) \\
&- 0.245038\,\mathcal{R}\left(R_7\right) - 0.0336275\,\mathcal{R}\left(R_8\right) + 3.44232\,\mathcal{R}\left(R_9\right) \\
&- 0.571287\,\mathcal{R}\left(R_{10}\right) + 3.00949 \Big] \times 10^{-7}, \quad\quad\quad\quad\quad\quad\quad\text{(B.4)}
\end{aligned}
$$

$$
\begin{aligned}
\mathcal{B}[1,3.5]_{\mu\mu} =\ & \Big[0.221569\,|R_7|^2 + 0.00297589\,|R_8|^2 + 0.800733\,|R_9|^2 \\
&+ 5.85121\,|R_{10}|^2 + 0.0173276\,\mathcal{I}\left(R_7 R_8^*\right) + 0.00288963\,\mathcal{I}\left(R_7 R_9^*\right) \\
&+ 0.0151859\,\mathcal{I}\left(R_8 R_9^*\right) - 0.000309907\,\mathcal{I}\left(R_8 R_{10}^*\right) + 0.0526479\,\mathcal{R}\left(R_7 R_8^*\right) \\
&- 0.503222\,\mathcal{R}\left(R_7 R_9^*\right) + 0.00893145\,\mathcal{R}\left(R_7 R_{10}^*\right) - 0.0585195\,\mathcal{R}\left(R_8 R_9^*\right) \\
&+ 0.00109835\,\mathcal{R}\left(R_8 R_{10}^*\right) - 0.0573964\,\mathcal{R}\left(R_9 R_{10}^*\right) + 0.018682\,\mathcal{I}\left(R_7\right) \\
&- 0.00307673\,\mathcal{I}\left(R_8\right) + 0.0461066\,\mathcal{I}\left(R_9\right) - 0.0020085\,\mathcal{I}\left(R_{10}\right) \\
&+ 0.170386\,\mathcal{R}\left(R_7\right) + 0.0103486\,\mathcal{R}\left(R_8\right) + 1.56162\,\mathcal{R}\left(R_9\right) \\
&- 0.296469\,\mathcal{R}\left(R_{10}\right) + 1.67348 \Big] \times 10^{-7}, \quad\quad\quad\quad\quad\quad\quad\text{(B.5)}
\end{aligned}
$$

$$
\begin{aligned}
\mathcal{B}[3.5,6]_{\mu\mu} =\ & \Big[0.0745453\,|R_7|^2 + 0.000916702\,|R_8|^2 + 0.724126\,|R_9|^2 \\
&+ 5.22861\,|R_{10}|^2 + 0.00587951\,\mathcal{I}\left(R_7 R_8^*\right) + 0.0021872\,\mathcal{I}\left(R_7 R_9^*\right) \\
&+ 0.0114944\,\mathcal{I}\left(R_8 R_9^*\right) - 0.000234573\,\mathcal{I}\left(R_8 R_{10}^*\right) + 0.0175166\,\mathcal{R}\left(R_7 R_8^*\right)
\end{aligned}
$$

$$
\begin{aligned}
&-0.371854\mathcal{R}\left(R_7 R_9^*\right)+0.00675653\mathcal{R}\left(R_7 R_{10}^*\right)-0.0416692\mathcal{R}\left(R_8 R_9^*\right)\\
&+0.000790901\mathcal{R}\left(R_8 R_{10}^*\right)-0.0524327\mathcal{R}\left(R_9 R_{10}^*\right)+0.0125784\mathcal{I}\left(R_7\right)\\
&+0.00944641\mathcal{I}\left(R_8\right)-0.00227977\mathcal{I}\left(R_9\right)-0.000977984\mathcal{I}\left(R_{10}\right)\\
&-0.360151\mathcal{R}\left(R_7\right)-0.0397297\mathcal{R}\left(R_8\right)+1.73717\mathcal{R}\left(R_9\right)\\
&-0.274818\mathcal{R}\left(R_{10}\right)+1.19972\Big]\times 10^{-7},
\end{aligned}\tag{B.6}
$$

$$
\begin{aligned}
\mathcal{B}[1,6]_{\mu\mu}=\Big[&0.296114\left|R_7\right|^2+0.00389259\left|R_8\right|^2+1.52486\left|R_9\right|^2\\
&+11.0798\left|R_{10}\right|^2+0.0232071\mathcal{I}\left(R_7 R_8^*\right)+0.00507683\mathcal{I}\left(R_7 R_9^*\right)\\
&+0.0266804\mathcal{I}\left(R_8 R_9^*\right)-0.00054448\mathcal{I}\left(R_8 R_{10}^*\right)+0.0701645\mathcal{R}\left(R_7 R_8^*\right)\\
&-0.875076\mathcal{R}\left(R_7 R_9^*\right)+0.015688\mathcal{R}\left(R_7 R_{10}^*\right)-0.100189\mathcal{R}\left(R_8 R_9^*\right)\\
&+0.00188925\mathcal{R}\left(R_8 R_{10}^*\right)-0.109829\mathcal{R}\left(R_9 R_{10}^*\right)+0.0312604\mathcal{I}\left(R_7\right)\\
&+0.00636967\mathcal{I}\left(R_8\right)+0.0438268\mathcal{I}\left(R_9\right)-0.00298649\mathcal{I}\left(R_{10}\right)\\
&-0.189764\mathcal{R}\left(R_7\right)-0.0293811\mathcal{R}\left(R_8\right)+3.29879\mathcal{R}\left(R_9\right)\\
&-0.571287\mathcal{R}\left(R_{10}\right)+2.8732\Big]\times 10^{-7},
\end{aligned}\tag{B.7}
$$

$$
\begin{aligned}
\mathcal{B}[1,3.5]_{\text{no em}}=\Big[&0.224822\left|R_7\right|^2+0.00299458\left|R_8\right|^2+0.785074\left|R_9\right|^2\\
&+5.68972\left|R_{10}\right|^2+0.0173276\mathcal{I}\left(R_7 R_8^*\right)+0.00288963\mathcal{I}\left(R_7 R_9^*\right)\\
&+0.0151859\mathcal{I}\left(R_8 R_9^*\right)-0.000309907\mathcal{I}\left(R_8 R_{10}^*\right)+0.053141\mathcal{R}\left(R_7 R_8^*\right)\\
&-0.49174\mathcal{R}\left(R_7 R_9^*\right)+0.00893145\mathcal{R}\left(R_7 R_{10}^*\right)-0.0576492\mathcal{R}\left(R_8 R_9^*\right)\\
&+0.00109835\mathcal{R}\left(R_8 R_{10}^*\right)-0.0573964\mathcal{R}\left(R_9 R_{10}^*\right)+0.0189329\mathcal{I}\left(R_7\right)\\
&-0.00305772\mathcal{I}\left(R_8\right)+0.0449044\mathcal{I}\left(R_9\right)-0.0020085\mathcal{I}\left(R_{10}\right)\\
&+0.202569\mathcal{R}\left(R_7\right)+0.0128309\mathcal{R}\left(R_8\right)+1.51378\mathcal{R}\left(R_9\right)\\
&-0.296469\mathcal{R}\left(R_{10}\right)+1.63384\Big]\times 10^{-7},
\end{aligned}\tag{B.8}
$$

$$
\begin{aligned}
\mathcal{B}[3.5,6]_{\text{no em}}=\Big[&0.0768325\left|R_7\right|^2+0.000929842\left|R_8\right|^2+0.717985\left|R_9\right|^2\\
&+5.19159\left|R_{10}\right|^2+0.00587951\mathcal{I}\left(R_7 R_8^*\right)+0.0021872\mathcal{I}\left(R_7 R_9^*\right)\\
&+0.0114944\mathcal{I}\left(R_8 R_9^*\right)-0.000234573\mathcal{I}\left(R_8 R_{10}^*\right)+0.0178634\mathcal{R}\left(R_7 R_8^*\right)\\
&-0.372512\mathcal{R}\left(R_7 R_9^*\right)+0.00675653\mathcal{R}\left(R_7 R_{10}^*\right)-0.0417191\mathcal{R}\left(R_8 R_9^*\right)\\
&+0.000790901\mathcal{R}\left(R_8 R_{10}^*\right)-0.0524327\mathcal{R}\left(R_9 R_{10}^*\right)+0.0129484\mathcal{I}\left(R_7\right)\\
&+0.00947445\mathcal{I}\left(R_8\right)-0.00403808\mathcal{I}\left(R_9\right)-0.000977984\mathcal{I}\left(R_{10}\right)\\
&-0.35297\mathcal{R}\left(R_7\right)-0.0391879\mathcal{R}\left(R_8\right)+1.70797\mathcal{R}\left(R_9\right)\\
&-0.274818\mathcal{R}\left(R_{10}\right)+1.16546\Big]\times 10^{-7},
\end{aligned}\tag{B.9}
$$

$$
\begin{aligned}
\mathcal{B}[1,6]_{\text{no em}}=\Big[&0.301655\left|R_7\right|^2+0.00392442\left|R_8\right|^2+1.50306\left|R_9\right|^2\\
&+10.8813\left|R_{10}\right|^2+0.0232071\mathcal{I}\left(R_7 R_8^*\right)+0.00507683\mathcal{I}\left(R_7 R_9^*\right)\\
&+0.0266804\mathcal{I}\left(R_8 R_9^*\right)-0.00054448\mathcal{I}\left(R_8 R_{10}^*\right)+0.0710044\mathcal{R}\left(R_7 R_8^*\right)\\
&-0.864251\mathcal{R}\left(R_7 R_9^*\right)+0.015688\mathcal{R}\left(R_7 R_{10}^*\right)-0.0993683\mathcal{R}\left(R_8 R_9^*\right)
\end{aligned}
$$

$$+0.00188925\mathcal{R}\left(R_8 R_{10}^*\right)-0.109829\mathcal{R}\left(R_9 R_{10}^*\right)+0.0318813\mathcal{I}\left(R_7\right)$$
$$+0.00641673\mathcal{I}\left(R_8\right)+0.0408664\mathcal{I}\left(R_9\right)-0.00298649\mathcal{I}\left(R_{10}\right)$$
$$-0.150401\mathcal{R}\left(R_7\right)-0.026357\mathcal{R}\left(R_8\right)+3.22175\mathcal{R}\left(R_9\right)$$
$$\left.-0.571287\mathcal{R}\left(R_{10}\right)+2.79931\right]\times 10^{-7}. \tag{B.10}$$

B.2 Branching ratio, high-q^2 region

$$\mathcal{B}[>14.4]_{ee}=\Big[0.000257481\mathcal{I}\left(R_7 R_8^*\right)+0.000385537\mathcal{I}\left(R_7 R_9^*\right)-0.0000314797\mathcal{I}\left(R_8 R_{10}^*\right)$$
$$+0.00154984\mathcal{I}\left(R_8 R_9^*\right)+0.000626787\mathcal{R}\left(R_7 R_8^*\right)-0.0448958\mathcal{R}\left(R_7 R_9^*\right)$$
$$-0.00499875\mathcal{R}\left(R_8 R_9^*\right)+0.00106976\mathcal{R}\left(R_7 R_{10}^*\right)-0.0163127\mathcal{R}\left(R_9 R_{10}^*\right)$$
$$+0.000114054\mathcal{R}\left(R_8 R_{10}^*\right)+0.00237824\left|R_7\right|^2+0.0000338564\left|R_8\right|^2$$
$$+0.190037\left|R_9\right|^2+1.3514\left|R_{10}\right|^2+0.00458151\mathcal{I}\left(R_7\right)$$
$$+0.00208694\mathcal{I}\left(R_8\right)+0.00740457\mathcal{I}\left(R_9\right)-0.000683152\mathcal{I}\left(R_{10}\right)$$
$$-0.0704095\mathcal{R}\left(R_7\right)-0.00781914\mathcal{R}\left(R_8\right)+0.497853\mathcal{R}\left(R_9\right)$$
$$\left.-0.0766318\mathcal{R}\left(R_{10}\right)+0.216631\right]\times 10^{-7}, \tag{B.11}$$
$$\mathcal{B}[>14.4]_{\mu\mu}=\Big[0.000257481\mathcal{I}\left(R_7 R_8^*\right)+0.000385537\mathcal{I}\left(R_7 R_9^*\right)-0.0000314797\mathcal{I}\left(R_8 R_{10}^*\right)$$
$$+0.00154984\mathcal{I}\left(R_8 R_9^*\right)+0.000756249\mathcal{R}\left(R_7 R_8^*\right)-0.0537067\mathcal{R}\left(R_7 R_9^*\right)$$
$$-0.00566659\mathcal{R}\left(R_8 R_9^*\right)+0.00106976\mathcal{R}\left(R_7 R_{10}^*\right)-0.0163127\mathcal{R}\left(R_9 R_{10}^*\right)$$
$$+0.000114054\mathcal{R}\left(R_8 R_{10}^*\right)+0.00323224\left|R_7\right|^2+0.0000387628\left|R_8\right|^2$$
$$+0.213448\left|R_9\right|^2+1.51361\left|R_{10}\right|^2+0.00272213\mathcal{I}\left(R_7\right)$$
$$+0.001946\mathcal{I}\left(R_8\right)+0.0173032\mathcal{I}\left(R_9\right)-0.000683152\mathcal{I}\left(R_{10}\right)$$
$$-0.0857515\mathcal{R}\left(R_7\right)-0.00901494\mathcal{R}\left(R_8\right)+0.58311\mathcal{R}\left(R_9\right)$$
$$\left.-0.0766318\mathcal{R}\left(R_{10}\right)+0.311364\right]\times 10^{-7}, \tag{B.12}$$
$$\mathcal{B}[>14.4]_{\text{no em}}=\Big[0.000257481\mathcal{I}\left(R_7 R_8^*\right)+0.000385537\mathcal{I}\left(R_7 R_9^*\right)-0.0000314797\mathcal{I}\left(R_8 R_{10}^*\right)$$
$$+0.00154984\mathcal{I}\left(R_8 R_9^*\right)+0.000848356\mathcal{R}\left(R_7 R_8^*\right)-0.0599752\mathcal{R}\left(R_7 R_9^*\right)$$
$$-0.00614173\mathcal{R}\left(R_8 R_9^*\right)+0.00106976\mathcal{R}\left(R_7 R_{10}^*\right)-0.0163127\mathcal{R}\left(R_9 R_{10}^*\right)$$
$$+0.000114054\mathcal{R}\left(R_8 R_{10}^*\right)+0.00383983\left|R_7\right|^2+0.0000422535\left|R_8\right|^2$$
$$+0.22634\left|R_9\right|^2+1.62902\left|R_{10}\right|^2+0.00139926\mathcal{I}\left(R_7\right)$$
$$+0.00184573\mathcal{I}\left(R_8\right)+0.0243456\mathcal{I}\left(R_9\right)-0.000683152\mathcal{I}\left(R_{10}\right)$$
$$-0.0966894\mathcal{R}\left(R_7\right)-0.00986742\mathcal{R}\left(R_8\right)+0.629448\mathcal{R}\left(R_9\right)$$
$$\left.-0.0766318\mathcal{R}\left(R_{10}\right)+0.364954\right]\times 10^{-7}. \tag{B.13}$$

B.3 The ratio $\mathcal{R}(s_0)$

$$
\begin{aligned}
\mathcal{R}(14.4)_{ee} = \Big[& 0.00345454\mathcal{I}\left(R_7 R_8^*\right) + 0.00518561\mathcal{I}\left(R_7 R_9^*\right) + 0.0204459\mathcal{I}\left(R_8 R_9^*\right) \\
& - 0.000422075\mathcal{I}\left(R_8 R_{10}^*\right) + 0.00769598\mathcal{R}\left(R_7 R_8^*\right) - 0.509477\mathcal{R}\left(R_7 R_9^*\right) \\
& - 0.0594276\mathcal{R}\left(R_8 R_9^*\right) + 0.0116279\mathcal{R}\left(R_7 R_{10}^*\right) + 0.00131861\mathcal{R}\left(R_8 R_{10}^*\right) \\
& - 0.178208\mathcal{R}\left(R_9 R_{10}^*\right) + 0.0274262\left|R_7\right|^2 + 0.000425936\left|R_8\right|^2 \\
& + 2.12663\left|R_9\right|^2 + 15.1222\left|R_{10}\right|^2 + 0.0610087\mathcal{I}\left(R_7\right) \\
& + 0.0240118\mathcal{I}\left(R_8\right) + 0.0219189\mathcal{I}\left(R_9\right) - 0.00627745\mathcal{I}\left(R_{10}\right) \\
& - 0.691986\mathcal{R}\left(R_7\right) - 0.0813958\mathcal{R}\left(R_8\right) + 4.65255\mathcal{R}\left(R_9\right) \\
& - 0.898911\mathcal{R}\left(R_{10}\right) + 1.99568 \Big] \times 10^{-4}\,,
\end{aligned}
\tag{B.14}
$$

$$
\begin{aligned}
\mathcal{R}(14.4)_{\mu\mu} = \Big[& 0.00345454\mathcal{I}\left(R_7 R_8^*\right) + 0.00518561\mathcal{I}\left(R_7 R_9^*\right) + 0.0204459\mathcal{I}\left(R_8 R_9^*\right) \\
& - 0.000422075\mathcal{I}\left(R_8 R_{10}^*\right) + 0.00925535\mathcal{R}\left(R_7 R_8^*\right) - 0.615603\mathcal{R}\left(R_7 R_9^*\right) \\
& - 0.0674718\mathcal{R}\left(R_8 R_9^*\right) + 0.0116279\mathcal{R}\left(R_7 R_{10}^*\right) + 0.00131861\mathcal{R}\left(R_8 R_{10}^*\right) \\
& - 0.178208\mathcal{R}\left(R_9 R_{10}^*\right) + 0.0377127\left|R_7\right|^2 + 0.000485034\left|R_8\right|^2 \\
& + 2.40861\left|R_9\right|^2 + 17.0761\left|R_{10}\right|^2 + 0.0386124\mathcal{I}\left(R_7\right) \\
& + 0.0223142\mathcal{I}\left(R_8\right) + 0.141148\mathcal{I}\left(R_9\right) - 0.00627745\mathcal{I}\left(R_{10}\right) \\
& - 0.852337\mathcal{R}\left(R_7\right) - 0.0939464\mathcal{R}\left(R_8\right) + 5.54958\mathcal{R}\left(R_9\right) \\
& - 0.898911\mathcal{R}\left(R_{10}\right) + 2.93907 \Big] \times 10^{-4}\,.
\end{aligned}
\tag{B.15}
$$

$$
\begin{aligned}
\mathcal{R}(14.4)_{\text{no em}} = \Big[& 0.00345454\mathcal{I}\left(R_7 R_8^*\right) + 0.00518561\mathcal{I}\left(R_7 R_9^*\right) + 0.0204459\mathcal{I}\left(R_8 R_9^*\right) \\
& - 0.000422075\mathcal{I}\left(R_8 R_{10}^*\right) + 0.0103648\mathcal{R}\left(R_7 R_8^*\right) - 0.691108\mathcal{R}\left(R_7 R_9^*\right) \\
& - 0.0731948\mathcal{R}\left(R_8 R_9^*\right) + 0.0116279\mathcal{R}\left(R_7 R_{10}^*\right) + 0.00131861\mathcal{R}\left(R_8 R_{10}^*\right) \\
& - 0.178208\mathcal{R}\left(R_9 R_{10}^*\right) + 0.045031\left|R_7\right|^2 + 0.00052708\left|R_8\right|^2 \\
& + 2.5639\left|R_9\right|^2 + 18.4662\left|R_{10}\right|^2 + 0.0226784\mathcal{I}\left(R_7\right) \\
& + 0.0211065\mathcal{I}\left(R_8\right) + 0.225975\mathcal{I}\left(R_9\right) - 0.00627745\mathcal{I}\left(R_{10}\right) \\
& - 0.966693\mathcal{R}\left(R_7\right) - 0.102896\mathcal{R}\left(R_8\right) + 6.03618\mathcal{R}\left(R_9\right) \\
& - 0.898911\mathcal{R}\left(R_{10}\right) + 3.47739 \Big] \times 10^{-4}\,.
\end{aligned}
\tag{B.16}
$$

B.4 Forward-backward asymmetry, low-q^2 region

$$
\begin{aligned}
\mathcal{H}_A[1, 3.5]_{ee} = \Big[& - 0.00177919\left|R_9\right|^2 - 0.0123279\left|R_{10}\right|^2 - 0.0000776477\mathcal{I}\left(R_8 R_9^*\right) \\
& + 0.0263923\mathcal{I}\left(R_8 R_{10}^*\right) + 0.00325843\mathcal{I}\left(R_9 R_{10}^*\right) + 0.00220437\mathcal{R}\left(R_7 R_9^*\right) \\
& - 0.870054\mathcal{R}\left(R_7 R_{10}^*\right) + 0.000227347\mathcal{R}\left(R_8 R_9^*\right) - 0.0864769\mathcal{R}\left(R_8 R_{10}^*\right) \\
& + 0.73759\mathcal{R}\left(R_9 R_{10}^*\right) - 0.0000857354\mathcal{I}\left(R_8\right) + 0.000225495\mathcal{I}\left(R_9\right) \\
& - 0.10319\mathcal{I}\left(R_{10}\right) + 0.023259\mathcal{R}\left(R_7\right) + 0.00182876\mathcal{R}\left(R_8\right) \\
& - 0.0136603\mathcal{R}\left(R_9\right) - 0.744674\mathcal{R}\left(R_{10}\right) + 0.0102674 \Big] \times 10^{-7}\,,
\end{aligned}
\tag{B.17}
$$

$$
\begin{aligned}
\mathcal{H}_A[3.5, 6]_{ee} = \Big[&- 0.0028283\,|R_9|^2 - 0.0195971\,|R_{10}|^2 - 0.0000582814\mathcal{I}\left(R_8 R_9^*\right) \\
&+ 0.0198099\mathcal{I}\left(R_8 R_{10}^*\right) + 0.00520128\mathcal{I}\left(R_9 R_{10}^*\right) + 0.00164717\mathcal{R}\left(R_7 R_9^*\right) \\
&- 0.620306\mathcal{R}\left(R_7 R_{10}^*\right) + 0.000173633\mathcal{R}\left(R_8 R_9^*\right) - 0.0636331\mathcal{R}\left(R_8 R_{10}^*\right) \\
&+ 1.10604\mathcal{R}\left(R_9 R_{10}^*\right) - 0.0000642074\mathcal{I}\left(R_8\right) + 0.000138567\mathcal{I}\left(R_9\right) \\
&- 0.0924194\mathcal{I}\left(R_{10}\right) + 0.0174663\mathcal{R}\left(R_7\right) + 0.00137799\mathcal{R}\left(R_8\right) \\
&- 0.0266284\mathcal{R}\left(R_9\right) + 0.533272\mathcal{R}\left(R_{10}\right) - 0.0149706 \Big] \times 10^{-7}, \quad \text{(B.18)}
\end{aligned}
$$

$$
\begin{aligned}
\mathcal{H}_A[1, 6]_{ee} = \Big[&- 0.00460749\,|R_9|^2 - 0.031925\,|R_{10}|^2 - 0.000135929\mathcal{I}\left(R_8 R_9^*\right) \\
&+ 0.0462021\mathcal{I}\left(R_8 R_{10}^*\right) + 0.00845971\mathcal{I}\left(R_9 R_{10}^*\right) + 0.00385155\mathcal{R}\left(R_7 R_9^*\right) \\
&- 1.49036\mathcal{R}\left(R_7 R_{10}^*\right) + 0.00040098\mathcal{R}\left(R_8 R_9^*\right) - 0.15011\mathcal{R}\left(R_8 R_{10}^*\right) \\
&+ 1.84363\mathcal{R}\left(R_9 R_{10}^*\right) - 0.000149943\mathcal{I}\left(R_8\right) + 0.000364062\mathcal{I}\left(R_9\right) \\
&- 0.19561\mathcal{I}\left(R_{10}\right) + 0.0407254\mathcal{R}\left(R_7\right) + 0.00320675\mathcal{R}\left(R_8\right) \\
&- 0.0402886\mathcal{R}\left(R_9\right) - 0.211402\mathcal{R}\left(R_{10}\right) - 0.0047032 \Big] \times 10^{-7}, \quad \text{(B.19)}
\end{aligned}
$$

$$
\begin{aligned}
\mathcal{H}_A[1, 3.5]_{\mu\mu} = \Big[&- 0.00177919\,|R_9|^2 - 0.0123279\,|R_{10}|^2 - 0.0000776477\mathcal{I}\left(R_8 R_9^*\right) \\
&+ 0.0263923\mathcal{I}\left(R_8 R_{10}^*\right) + 0.00325843\mathcal{I}\left(R_9 R_{10}^*\right) + 0.00220437\mathcal{R}\left(R_7 R_9^*\right) \\
&- 0.86614\mathcal{R}\left(R_7 R_{10}^*\right) + 0.000227347\mathcal{R}\left(R_8 R_9^*\right) - 0.0861802\mathcal{R}\left(R_8 R_{10}^*\right) \\
&+ 0.708627\mathcal{R}\left(R_9 R_{10}^*\right) - 0.0000857354\mathcal{I}\left(R_8\right) + 0.000225495\mathcal{I}\left(R_9\right) \\
&- 0.10319\mathcal{I}\left(R_{10}\right) + 0.023259\mathcal{R}\left(R_7\right) + 0.00182876\mathcal{R}\left(R_8\right) \\
&- 0.0136603\mathcal{R}\left(R_9\right) - 0.79481\mathcal{R}\left(R_{10}\right) + 0.0112923 \Big] \times 10^{-7}, \quad \text{(B.20)}
\end{aligned}
$$

$$
\begin{aligned}
\mathcal{H}_A[3.5, 6]_{\mu\mu} = \Big[&- 0.0028283\,|R_9|^2 - 0.0195971\,|R_{10}|^2 - 0.0000582814\mathcal{I}\left(R_8 R_9^*\right) \\
&+ 0.0198099\mathcal{I}\left(R_8 R_{10}^*\right) + 0.00520128\mathcal{I}\left(R_9 R_{10}^*\right) + 0.00164717\mathcal{R}\left(R_7 R_9^*\right) \\
&- 0.635041\mathcal{R}\left(R_7 R_{10}^*\right) + 0.000173633\mathcal{R}\left(R_8 R_9^*\right) - 0.0647501\mathcal{R}\left(R_8 R_{10}^*\right) \\
&+ 1.09972\mathcal{R}\left(R_9 R_{10}^*\right) - 0.0000642074\mathcal{I}\left(R_8\right) + 0.000138567\mathcal{I}\left(R_9\right) \\
&- 0.092495\mathcal{I}\left(R_{10}\right) + 0.0174663\mathcal{R}\left(R_7\right) + 0.00137799\mathcal{R}\left(R_8\right) \\
&- 0.0266284\mathcal{R}\left(R_9\right) + 0.494194\mathcal{R}\left(R_{10}\right) - 0.0147469 \Big] \times 10^{-7}, \quad \text{(B.21)}
\end{aligned}
$$

$$
\begin{aligned}
\mathcal{H}_A[1, 6]_{\mu\mu} = \Big[&- 0.00460749\,|R_9|^2 - 0.031925\,|R_{10}|^2 - 0.000135929\mathcal{I}\left(R_8 R_9^*\right) \\
&+ 0.0462021\mathcal{I}\left(R_8 R_{10}^*\right) + 0.00845971\mathcal{I}\left(R_9 R_{10}^*\right) + 0.00385155\mathcal{R}\left(R_7 R_9^*\right) \\
&- 1.50118\mathcal{R}\left(R_7 R_{10}^*\right) + 0.00040098\mathcal{R}\left(R_8 R_9^*\right) - 0.15093\mathcal{R}\left(R_8 R_{10}^*\right) \\
&+ 1.80835\mathcal{R}\left(R_9 R_{10}^*\right) - 0.000149943\mathcal{I}\left(R_8\right) + 0.000364062\mathcal{I}\left(R_9\right) \\
&- 0.195685\mathcal{I}\left(R_{10}\right) + 0.0407254\mathcal{R}\left(R_7\right) + 0.00320675\mathcal{R}\left(R_8\right) \\
&- 0.0402886\mathcal{R}\left(R_9\right) - 0.300616\mathcal{R}\left(R_{10}\right) - 0.00345465 \Big] \times 10^{-7}, \quad \text{(B.22)}
\end{aligned}
$$

$$
\begin{aligned}
\mathcal{H}_A[1, 3.5]_{\text{no em}} = \Big[&- 0.00177919\,|R_9|^2 - 0.0123279\,|R_{10}|^2 - 0.0000776477\mathcal{I}\left(R_8 R_9^*\right) \\
&+ 0.0263923\mathcal{I}\left(R_8 R_{10}^*\right) + 0.00325843\mathcal{I}\left(R_9 R_{10}^*\right) + 0.00220437\mathcal{R}\left(R_7 R_9^*\right)
\end{aligned}
$$

$$\begin{aligned}
&\quad - 0.863355\mathcal{R}\left(R_7 R_{10}^*\right) + 0.000227347\mathcal{R}\left(R_8 R_9^*\right) - 0.0859692\mathcal{R}\left(R_8 R_{10}^*\right)\\
&\quad + 0.688022\mathcal{R}\left(R_9 R_{10}^*\right) - 0.0000857354\mathcal{I}\left(R_8\right) + 0.000225495\mathcal{I}\left(R_9\right)\\
&\quad - 0.10319\mathcal{I}\left(R_{10}\right) + 0.023259\mathcal{R}\left(R_7\right) + 0.00182876\mathcal{R}\left(R_8\right)\\
&\quad - 0.0136603\mathcal{R}\left(R_9\right) - 0.830553\mathcal{R}\left(R_{10}\right) + 0.0120214 \Big] \times 10^{-7}, \quad \text{(B.23)}
\end{aligned}$$

$$\begin{aligned}
\mathcal{H}_A[3.5,6]_{\text{no em}} =& \Big[- 0.0028283\left|R_9\right|^2 - 0.0195971\left|R_{10}\right|^2 - 0.0000582814\mathcal{I}\left(R_8 R_9^*\right)\\
&+ 0.0198099\mathcal{I}\left(R_8 R_{10}^*\right) + 0.00520128\mathcal{I}\left(R_9 R_{10}^*\right) + 0.00164717\mathcal{R}\left(R_7 R_9^*\right)\\
&- 0.645525\mathcal{R}\left(R_7 R_{10}^*\right) + 0.000173633\mathcal{R}\left(R_8 R_9^*\right) - 0.0655447\mathcal{R}\left(R_8 R_{10}^*\right)\\
&+ 1.09522\mathcal{R}\left(R_9 R_{10}^*\right) - 0.0000642074\mathcal{I}\left(R_8\right) + 0.000138567\mathcal{I}\left(R_9\right)\\
&- 0.0925487\mathcal{I}\left(R_{10}\right) + 0.0174663\mathcal{R}\left(R_7\right) + 0.00137799\mathcal{R}\left(R_8\right)\\
&- 0.0266284\mathcal{R}\left(R_9\right) + 0.466375\mathcal{R}\left(R_{10}\right) - 0.0145878 \Big] \times 10^{-7}, \quad \text{(B.24)}
\end{aligned}$$

$$\begin{aligned}
\mathcal{H}_A[1,6]_{\text{no em}} =& \Big[- 0.00460749\left|R_9\right|^2 - 0.031925\left|R_{10}\right|^2 - 0.000135929\mathcal{I}\left(R_8 R_9^*\right)\\
&+ 0.0462021\mathcal{I}\left(R_8 R_{10}^*\right) + 0.00845971\mathcal{I}\left(R_9 R_{10}^*\right) + 0.00385155\mathcal{R}\left(R_7 R_9^*\right)\\
&- 1.50888\mathcal{R}\left(R_7 R_{10}^*\right) + 0.00040098\mathcal{R}\left(R_8 R_9^*\right) - 0.151514\mathcal{R}\left(R_8 R_{10}^*\right)\\
&+ 1.78325\mathcal{R}\left(R_9 R_{10}^*\right) - 0.000149943\mathcal{I}\left(R_8\right) + 0.000364062\mathcal{I}\left(R_9\right)\\
&- 0.195739\mathcal{I}\left(R_{10}\right) + 0.0407254\mathcal{R}\left(R_7\right) + 0.00320675\mathcal{R}\left(R_8\right)\\
&- 0.0402886\mathcal{R}\left(R_9\right) - 0.364178\mathcal{R}\left(R_{10}\right) - 0.00256636 \Big] \times 10^{-7}. \quad \text{(B.25)}
\end{aligned}$$

B.5 H_L and H_T, low-q^2 region

$$\begin{aligned}
\mathcal{H}_L[1,3.5]_{ee} =& \Big[0.000747411\mathcal{I}\left(R_7 R_8^*\right) + 0.000977063\mathcal{I}\left(R_7 R_9^*\right) + 0.00513472\mathcal{I}\left(R_8 R_9^*\right)\\
&- 0.000104788\mathcal{I}\left(R_8 R_{10}^*\right) + 0.00214866\mathcal{R}\left(R_7 R_8^*\right) - 0.140096\mathcal{R}\left(R_7 R_9^*\right)\\
&- 0.0191872\mathcal{R}\left(R_8 R_9^*\right) + 0.00308685\mathcal{R}\left(R_7 R_{10}^*\right) - 0.047482\mathcal{R}\left(R_9 R_{10}^*\right)\\
&+ 0.000411202\mathcal{R}\left(R_8 R_{10}^*\right) + 0.00586189\left|R_7\right|^2 + 0.00012925\left|R_8\right|^2\\
&+ 0.591901\left|R_9\right|^2 + 4.30913\left|R_{10}\right|^2 - 0.00448177\mathcal{I}\left(R_7\right)\\
&+ 0.00578567\mathcal{I}\left(R_8\right) + 0.0501124\mathcal{I}\left(R_9\right) - 0.00204632\mathcal{I}\left(R_{10}\right)\\
&- 0.218574\mathcal{R}\left(R_7\right) - 0.0279545\mathcal{R}\left(R_8\right) + 1.59319\mathcal{R}\left(R_9\right)\\
&- 0.257169\mathcal{R}\left(R_{10}\right) + 1.12382 \Big] \times 10^{-7}, \quad \text{(B.26)}
\end{aligned}$$

$$\begin{aligned}
\mathcal{H}_L[3.5,6]_{ee} =& \Big[0.000564413\mathcal{I}\left(R_7 R_8^*\right) + 0.000742411\mathcal{I}\left(R_7 R_9^*\right) + 0.00390158\mathcal{I}\left(R_8 R_9^*\right)\\
&- 0.0000796221\mathcal{I}\left(R_8 R_{10}^*\right) + 0.00176752\mathcal{R}\left(R_7 R_8^*\right) - 0.110436\mathcal{R}\left(R_7 R_9^*\right)\\
&- 0.0139287\mathcal{R}\left(R_8 R_9^*\right) + 0.00234522\mathcal{R}\left(R_7 R_{10}^*\right) + 0.000292701\mathcal{R}\left(R_8 R_{10}^*\right)\\
&- 0.0365245\mathcal{R}\left(R_9 R_{10}^*\right) + 0.00629886\left|R_7\right|^2 + 0.0000978272\left|R_8\right|^2\\
&+ 0.453059\left|R_9\right|^2 + 3.29103\left|R_{10}\right|^2 + 0.00231621\mathcal{I}\left(R_7\right)\\
&+ 0.00530567\mathcal{I}\left(R_8\right) - 0.0014697\mathcal{I}\left(R_9\right) - 0.000854216\mathcal{I}\left(R_{10}\right)
\end{aligned}$$

$$
\begin{aligned}
&- 0.184255\mathcal{R}\left(R_7\right) - 0.0217067\mathcal{R}\left(R_8\right) + 1.31804\mathcal{R}\left(R_9\right) \\
&\left.- 0.198876\mathcal{R}\left(R_{10}\right) + 0.92649\right] \times 10^{-7}\,,
\end{aligned} \tag{B.27}
$$

$$
\begin{aligned}
\mathcal{H}_L[1,6]_{ee} = \Big[&0.00131182\mathcal{I}\left(R_7 R_8^*\right) + 0.00171947\mathcal{I}\left(R_7 R_9^*\right) + 0.0090363\mathcal{I}\left(R_8 R_9^*\right) \\
&- 0.00018441\mathcal{I}\left(R_8 R_{10}^*\right) + 0.00391618\mathcal{R}\left(R_7 R_8^*\right) - 0.250532\mathcal{R}\left(R_7 R_9^*\right) \\
&- 0.0331159\mathcal{R}\left(R_8 R_9^*\right) + 0.00543208\mathcal{R}\left(R_7 R_{10}^*\right) + 0.000703903\mathcal{R}\left(R_8 R_{10}^*\right) \\
&- 0.0840066\mathcal{R}\left(R_9 R_{10}^*\right) + 0.0121607\left|R_7\right|^2 + 0.000227077\left|R_8\right|^2 \\
&+ 1.04496\left|R_9\right|^2 + 7.60015\left|R_{10}\right|^2 - 0.00216555\mathcal{I}\left(R_7\right) \\
&+ 0.0110913\mathcal{I}\left(R_8\right) + 0.0486427\mathcal{I}\left(R_9\right) - 0.00290053\mathcal{I}\left(R_{10}\right) \\
&- 0.402829\mathcal{R}\left(R_7\right) - 0.0496612\mathcal{R}\left(R_8\right) + 2.91123\mathcal{R}\left(R_9\right) \\
&\left.- 0.456045\mathcal{R}\left(R_{10}\right) + 2.05031\right] \times 10^{-7}\,,
\end{aligned} \tag{B.28}
$$

$$
\begin{aligned}
\mathcal{H}_L[1,3.5]_{\mu\mu} = \Big[&0.000747411\mathcal{I}\left(R_7 R_8^*\right) + 0.000977063\mathcal{I}\left(R_7 R_9^*\right) + 0.00513472\mathcal{I}\left(R_8 R_9^*\right) \\
&- 0.000104788\mathcal{I}\left(R_8 R_{10}^*\right) + 0.00262758\mathcal{R}\left(R_7 R_8^*\right) - 0.15727\mathcal{R}\left(R_7 R_9^*\right) \\
&- 0.020489\mathcal{R}\left(R_8 R_9^*\right) + 0.00308685\mathcal{R}\left(R_7 R_{10}^*\right) + 0.000411202\mathcal{R}\left(R_8 R_{10}^*\right) \\
&- 0.047482\mathcal{R}\left(R_9 R_{10}^*\right) + 0.0090211\left|R_7\right|^2 + 0.0001474\left|R_8\right|^2 \\
&+ 0.625902\left|R_9\right|^2 + 4.54472\left|R_{10}\right|^2 - 0.00541775\mathcal{I}\left(R_7\right) \\
&+ 0.00571472\mathcal{I}\left(R_8\right) + 0.0546139\mathcal{I}\left(R_9\right) - 0.00204632\mathcal{I}\left(R_{10}\right) \\
&- 0.241612\mathcal{R}\left(R_7\right) - 0.0297648\mathcal{R}\left(R_8\right) + 1.70159\mathcal{R}\left(R_9\right) \\
&\left.- 0.257169\mathcal{R}\left(R_{10}\right) + 1.23483\right] \times 10^{-7}\,,
\end{aligned} \tag{B.29}
$$

$$
\begin{aligned}
\mathcal{H}_L[3.5,6]_{\mu\mu} = \Big[&0.000564413\mathcal{I}\left(R_7 R_8^*\right) + 0.000742411\mathcal{I}\left(R_7 R_9^*\right) + 0.00390158\mathcal{I}\left(R_8 R_9^*\right) \\
&- 0.0000796221\mathcal{I}\left(R_8 R_{10}^*\right) + 0.00195014\mathcal{R}\left(R_7 R_8^*\right) - 0.121246\mathcal{R}\left(R_7 R_9^*\right) \\
&- 0.0147481\mathcal{R}\left(R_8 R_9^*\right) + 0.00234522\mathcal{R}\left(R_7 R_{10}^*\right) + 0.000292701\mathcal{R}\left(R_8 R_{10}^*\right) \\
&- 0.0365245\mathcal{R}\left(R_9 R_{10}^*\right) + 0.00750349\left|R_7\right|^2 + 0.000104748\left|R_8\right|^2 \\
&+ 0.480992\left|R_9\right|^2 + 3.48458\left|R_{10}\right|^2 + 0.00137075\mathcal{I}\left(R_7\right) \\
&+ 0.005234\mathcal{I}\left(R_8\right) + 0.00314813\mathcal{I}\left(R_9\right) - 0.000854216\mathcal{I}\left(R_{10}\right) \\
&- 0.200992\mathcal{R}\left(R_7\right) - 0.0230157\mathcal{R}\left(R_8\right) + 1.41053\mathcal{R}\left(R_9\right) \\
&\left.- 0.198876\mathcal{R}\left(R_{10}\right) + 1.01906\right] \times 10^{-7}\,,
\end{aligned} \tag{B.30}
$$

$$
\begin{aligned}
\mathcal{H}_L[1,6]_{\mu\mu} = \Big[&0.00131182\mathcal{I}\left(R_7 R_8^*\right) + 0.00171947\mathcal{I}\left(R_7 R_9^*\right) + 0.0090363\mathcal{I}\left(R_8 R_9^*\right) \\
&- 0.00018441\mathcal{I}\left(R_8 R_{10}^*\right) + 0.00457772\mathcal{R}\left(R_7 R_8^*\right) - 0.278516\mathcal{R}\left(R_7 R_9^*\right) \\
&- 0.0352371\mathcal{R}\left(R_8 R_9^*\right) + 0.00543208\mathcal{R}\left(R_7 R_{10}^*\right) + 0.000703903\mathcal{R}\left(R_8 R_{10}^*\right) \\
&- 0.0840066\mathcal{R}\left(R_9 R_{10}^*\right) + 0.0165246\left|R_7\right|^2 + 0.000252149\left|R_8\right|^2 \\
&+ 1.10689\left|R_9\right|^2 + 8.02929\left|R_{10}\right|^2 - 0.004047\mathcal{I}\left(R_7\right) \\
&+ 0.0109487\mathcal{I}\left(R_8\right) + 0.0577621\mathcal{I}\left(R_9\right) - 0.00290053\mathcal{I}\left(R_{10}\right)
\end{aligned}
$$

$$
\begin{aligned}
&\quad - 0.442604\mathcal{R}\left(R_7\right) - 0.0527806\mathcal{R}\left(R_8\right) + 3.11211\mathcal{R}\left(R_9\right) \\
&\quad - 0.456045\mathcal{R}\left(R_{10}\right) + 2.25389 \Big] \times 10^{-7}\,, \tag{B.31}
\end{aligned}
$$

$$
\begin{aligned}
\mathcal{H}_L[1,3.5]_{\text{no em}} =\ & \Big[0.000747411\mathcal{I}\left(R_7 R_8^*\right) + 0.000977063\mathcal{I}\left(R_7 R_9^*\right) + 0.00513472\mathcal{I}\left(R_8 R_9^*\right) \\
&\quad - 0.000104788\mathcal{I}\left(R_8 R_{10}^*\right) + 0.00296831\mathcal{R}\left(R_7 R_8^*\right) - 0.169489\mathcal{R}\left(R_7 R_9^*\right) \\
&\quad - 0.0214151\mathcal{R}\left(R_8 R_9^*\right) + 0.00308685\mathcal{R}\left(R_7 R_{10}^*\right) + 0.000411202\mathcal{R}\left(R_8 R_{10}^*\right) \\
&\quad - 0.047482\mathcal{R}\left(R_9 R_{10}^*\right) + 0.0112687\left|R_7\right|^2 + 0.000160314\left|R_8\right|^2 \\
&\quad + 0.650092\left|R_9\right|^2 + 4.71233\left|R_{10}\right|^2 - 0.00608367\mathcal{I}\left(R_7\right) \\
&\quad + 0.00566425\mathcal{I}\left(R_8\right) + 0.0578166\mathcal{I}\left(R_9\right) - 0.00204632\mathcal{I}\left(R_{10}\right) \\
&\quad - 0.258047\mathcal{R}\left(R_7\right) - 0.0310562\mathcal{R}\left(R_8\right) + 1.77889\mathcal{R}\left(R_9\right) \\
&\quad - 0.257169\mathcal{R}\left(R_{10}\right) + 1.31413 \Big] \times 10^{-7}\,, \tag{B.32}
\end{aligned}
$$

$$
\begin{aligned}
\mathcal{H}_L[3.5,6]_{\text{no em}} =\ & \Big[0.000564413\mathcal{I}\left(R_7 R_8^*\right) + 0.000742411\mathcal{I}\left(R_7 R_9^*\right) + 0.00390158\mathcal{I}\left(R_8 R_9^*\right) \\
&\quad - 0.0000796221\mathcal{I}\left(R_8 R_{10}^*\right) + 0.00208006\mathcal{R}\left(R_7 R_8^*\right) - 0.128937\mathcal{R}\left(R_7 R_9^*\right) \\
&\quad - 0.015331\mathcal{R}\left(R_8 R_9^*\right) + 0.00234522\mathcal{R}\left(R_7 R_{10}^*\right) + 0.000292701\mathcal{R}\left(R_8 R_{10}^*\right) \\
&\quad - 0.0365245\mathcal{R}\left(R_9 R_{10}^*\right) + 0.00836054\left|R_7\right|^2 + 0.000109672\left|R_8\right|^2 \\
&\quad + 0.500866\left|R_9\right|^2 + 3.62228\left|R_{10}\right|^2 + 0.000698096\mathcal{I}\left(R_7\right) \\
&\quad + 0.00518302\mathcal{I}\left(R_8\right) + 0.0064335\mathcal{I}\left(R_9\right) - 0.000854216\mathcal{I}\left(R_{10}\right) \\
&\quad - 0.212928\mathcal{R}\left(R_7\right) - 0.0239492\mathcal{R}\left(R_8\right) + 1.47647\mathcal{R}\left(R_9\right) \\
&\quad - 0.198876\mathcal{R}\left(R_{10}\right) + 1.08519 \Big] \times 10^{-7}\,, \tag{B.33}
\end{aligned}
$$

$$
\begin{aligned}
\mathcal{H}_L[1,6]_{\text{no em}} =\ & \Big[0.00131182\mathcal{I}\left(R_7 R_8^*\right) + 0.00171947\mathcal{I}\left(R_7 R_9^*\right) + 0.0090363\mathcal{I}\left(R_8 R_9^*\right) \\
&\quad - 0.00018441\mathcal{I}\left(R_8 R_{10}^*\right) + 0.00504837\mathcal{R}\left(R_7 R_8^*\right) - 0.298426\mathcal{R}\left(R_7 R_9^*\right) \\
&\quad - 0.0367462\mathcal{R}\left(R_8 R_9^*\right) + 0.00543208\mathcal{R}\left(R_7 R_{10}^*\right) + 0.000703903\mathcal{R}\left(R_8 R_{10}^*\right) \\
&\quad - 0.0840066\mathcal{R}\left(R_9 R_{10}^*\right) + 0.0196293\left|R_7\right|^2 + 0.000269986\left|R_8\right|^2 \\
&\quad + 1.15096\left|R_9\right|^2 + 8.33461\left|R_{10}\right|^2 - 0.00538557\mathcal{I}\left(R_7\right) \\
&\quad + 0.0108473\mathcal{I}\left(R_8\right) + 0.0642501\mathcal{I}\left(R_9\right) - 0.00290053\mathcal{I}\left(R_{10}\right) \\
&\quad - 0.470975\mathcal{R}\left(R_7\right) - 0.0550053\mathcal{R}\left(R_8\right) + 3.25535\mathcal{R}\left(R_9\right) \\
&\quad - 0.456045\mathcal{R}\left(R_{10}\right) + 2.39933 \Big] \times 10^{-7}\,. \tag{B.34}
\end{aligned}
$$

$$
\begin{aligned}
\mathcal{H}_T[1,3.5]_{ee} =\ & \Big[0.0165802\mathcal{I}\left(R_7 R_8^*\right) + 0.00191257\mathcal{I}\left(R_7 R_9^*\right) + 0.0100512\mathcal{I}\left(R_8 R_9^*\right) \\
&\quad - 0.000205119\mathcal{I}\left(R_8 R_{10}^*\right) + 0.0469885\mathcal{R}\left(R_7 R_8^*\right) - 0.379261\mathcal{R}\left(R_7 R_9^*\right) \\
&\quad - 0.0377252\mathcal{R}\left(R_8 R_9^*\right) + 0.0058446\mathcal{R}\left(R_7 R_{10}^*\right) + 0.000628542\mathcal{R}\left(R_8 R_{10}^*\right) \\
&\quad - 0.00991432\mathcal{R}\left(R_9 R_{10}^*\right) + 0.211135\left|R_7\right|^2 + 0.00234936\left|R_8\right|^2 \\
&\quad + 0.249236\left|R_9\right|^2 + 1.76904\left|R_{10}\right|^2 + 0.0362042\mathcal{I}\left(R_7\right) \\
&\quad - 0.00833705\mathcal{I}\left(R_8\right) - 0.0146216\mathcal{I}\left(R_9\right) + 0.000290922\mathcal{I}\left(R_{10}\right)
\end{aligned}
$$

$$
\begin{aligned}
&+ 0.352468\mathcal{R}\left(R_7\right) + 0.03572\mathcal{R}\left(R_8\right) + 0.0901749\mathcal{R}\left(R_9\right) \\
&- 0.0390521\mathcal{R}\left(R_{10}\right) + 0.614659 \Big] \times 10^{-7}\,, \tag{B.35}
\end{aligned}
$$

$$
\begin{aligned}
\mathcal{H}_T[3.5,6]_{ee} = \Big[&0.0053151\mathcal{I}\left(R_7 R_8^*\right) + 0.00144479\mathcal{I}\left(R_7 R_9^*\right) + 0.00759287\mathcal{I}\left(R_8 R_9^*\right) \\
&- 0.00015495\mathcal{I}\left(R_8 R_{10}^*\right) + 0.0147212\mathcal{R}\left(R_7 R_8^*\right) - 0.260494\mathcal{R}\left(R_7 R_9^*\right) \\
&- 0.0266142\mathcal{R}\left(R_8 R_9^*\right) + 0.0044113\mathcal{R}\left(R_7 R_{10}^*\right) + 0.000476328\mathcal{R}\left(R_8 R_{10}^*\right) \\
&- 0.0159082\mathcal{R}\left(R_9 R_{10}^*\right) + 0.0650316\left|R_7\right|^2 + 0.00074246\left|R_8\right|^2 \\
&+ 0.27778\left|R_9\right|^2 + 1.98963\left|R_{10}\right|^2 + 0.0155002\mathcal{I}\left(R_7\right) \\
&+ 0.00455726\mathcal{I}\left(R_8\right) - 0.00974966\mathcal{I}\left(R_9\right) + 0.000110893\mathcal{I}\left(R_{10}\right) \\
&- 0.181332\mathcal{R}\left(R_7\right) - 0.0172841\mathcal{R}\left(R_8\right) + 0.443444\mathcal{R}\left(R_9\right) \\
&- 0.0757004\mathcal{R}\left(R_{10}\right) + 0.292097 \Big] \times 10^{-7}\,, \tag{B.36}
\end{aligned}
$$

$$
\begin{aligned}
\mathcal{H}_T[1,6]_{ee} = \Big[&0.0218953\mathcal{I}\left(R_7 R_8^*\right) + 0.00335736\mathcal{I}\left(R_7 R_9^*\right) + 0.017644\mathcal{I}\left(R_8 R_9^*\right) \\
&- 0.00036007\mathcal{I}\left(R_8 R_{10}^*\right) + 0.0617098\mathcal{R}\left(R_7 R_8^*\right) - 0.639755\mathcal{R}\left(R_7 R_9^*\right) \\
&- 0.0643394\mathcal{R}\left(R_8 R_9^*\right) + 0.0102559\mathcal{R}\left(R_7 R_{10}^*\right) + 0.00110487\mathcal{R}\left(R_8 R_{10}^*\right) \\
&- 0.0258225\mathcal{R}\left(R_9 R_{10}^*\right) + 0.276167\left|R_7\right|^2 + 0.00309182\left|R_8\right|^2 \\
&+ 0.527016\left|R_9\right|^2 + 3.75867\left|R_{10}\right|^2 + 0.0517044\mathcal{I}\left(R_7\right) \\
&- 0.00377979\mathcal{I}\left(R_8\right) - 0.0243713\mathcal{I}\left(R_9\right) + 0.000401815\mathcal{I}\left(R_{10}\right) \\
&+ 0.171135\mathcal{R}\left(R_7\right) + 0.018436\mathcal{R}\left(R_8\right) + 0.533619\mathcal{R}\left(R_9\right) \\
&- 0.114753\mathcal{R}\left(R_{10}\right) + 0.906757 \Big] \times 10^{-7}\,, \tag{B.37}
\end{aligned}
$$

$$
\begin{aligned}
\mathcal{H}_T[1,3.5]_{\mu\mu} = \Big[&0.0165802\mathcal{I}\left(R_7 R_8^*\right) + 0.00191257\mathcal{I}\left(R_7 R_9^*\right) + 0.0100512\mathcal{I}\left(R_8 R_9^*\right) \\
&- 0.000205119\mathcal{I}\left(R_8 R_{10}^*\right) + 0.0472027\mathcal{R}\left(R_7 R_8^*\right) - 0.34595\mathcal{R}\left(R_7 R_9^*\right) \\
&- 0.0352003\mathcal{R}\left(R_8 R_9^*\right) + 0.0058446\mathcal{R}\left(R_7 R_{10}^*\right) + 0.000628542\mathcal{R}\left(R_8 R_{10}^*\right) \\
&- 0.00991432\mathcal{R}\left(R_9 R_{10}^*\right) + 0.212548\left|R_7\right|^2 + 0.00235748\left|R_8\right|^2 \\
&+ 0.182478\left|R_9\right|^2 + 1.30648\left|R_{10}\right|^2 + 0.0374908\mathcal{I}\left(R_7\right) \\
&- 0.00823953\mathcal{I}\left(R_8\right) - 0.0208026\mathcal{I}\left(R_9\right) + 0.000290922\mathcal{I}\left(R_{10}\right) \\
&+ 0.420669\mathcal{R}\left(R_7\right) + 0.0410139\mathcal{R}\left(R_8\right) - 0.12403\mathcal{R}\left(R_9\right) \\
&- 0.0390521\mathcal{R}\left(R_{10}\right) + 0.413317 \Big] \times 10^{-7}\,, \tag{B.38}
\end{aligned}
$$

$$
\begin{aligned}
\mathcal{H}_T[3.5,6]_{\mu\mu} = \Big[&0.0053151\mathcal{I}\left(R_7 R_8^*\right) + 0.00144479\mathcal{I}\left(R_7 R_9^*\right) + 0.00759287\mathcal{I}\left(R_8 R_9^*\right) \\
&- 0.00015495\mathcal{I}\left(R_8 R_{10}^*\right) + 0.015026\mathcal{R}\left(R_7 R_8^*\right) - 0.250608\mathcal{R}\left(R_7 R_9^*\right) \\
&- 0.0258649\mathcal{R}\left(R_8 R_9^*\right) + 0.0044113\mathcal{R}\left(R_7 R_{10}^*\right) + 0.000476328\mathcal{R}\left(R_8 R_{10}^*\right) \\
&- 0.0159082\mathcal{R}\left(R_9 R_{10}^*\right) + 0.0670418\left|R_7\right|^2 + 0.000754009\left|R_8\right|^2 \\
&+ 0.242336\left|R_9\right|^2 + 1.74404\left|R_{10}\right|^2 + 0.0169642\mathcal{I}\left(R_7\right) \\
&+ 0.00466823\mathcal{I}\left(R_8\right) - 0.0168279\mathcal{I}\left(R_9\right) + 0.000110893\mathcal{I}\left(R_{10}\right)
\end{aligned}
$$

$$
\begin{aligned}
&\quad - 0.154501\mathcal{R}\left(R_7\right) - 0.0152134\mathcal{R}\left(R_8\right) + 0.313295\mathcal{R}\left(R_9\right) \\
&\quad \left. - 0.0757004\mathcal{R}\left(R_{10}\right) + 0.153748\right] \times 10^{-7}\,, \tag{B.39}
\end{aligned}
$$

$$
\begin{aligned}
\mathcal{H}_T[1,6]_{\mu\mu} = &\Big[0.0218953\mathcal{I}\left(R_7 R_8^*\right) + 0.00335736\mathcal{I}\left(R_7 R_9^*\right) + 0.017644\mathcal{I}\left(R_8 R_9^*\right) \\
&- 0.00036007\mathcal{I}\left(R_8 R_{10}^*\right) + 0.0622287\mathcal{R}\left(R_7 R_8^*\right) - 0.596558\mathcal{R}\left(R_7 R_9^*\right) \\
&- 0.0610652\mathcal{R}\left(R_8 R_9^*\right) + 0.0102559\mathcal{R}\left(R_7 R_{10}^*\right) + 0.00110487\mathcal{R}\left(R_8 R_{10}^*\right) \\
&- 0.0258225\mathcal{R}\left(R_9 R_{10}^*\right) + 0.27959\left|R_7\right|^2 + 0.00311149\left|R_8\right|^2 \\
&+ 0.424814\left|R_9\right|^2 + 3.05052\left|R_{10}\right|^2 + 0.054455\mathcal{I}\left(R_7\right) \\
&- 0.0035713\mathcal{I}\left(R_8\right) - 0.0376305\mathcal{I}\left(R_9\right) + 0.000401815\mathcal{I}\left(R_{10}\right) \\
&+ 0.266168\mathcal{R}\left(R_7\right) + 0.0258005\mathcal{R}\left(R_8\right) + 0.189265\mathcal{R}\left(R_9\right) \\
&\left. - 0.114753\mathcal{R}\left(R_{10}\right) + 0.567065\right] \times 10^{-7}\,, \tag{B.40}
\end{aligned}
$$

$$
\begin{aligned}
\mathcal{H}_T[1,3.5]_{\text{no em}} = &\Big[0.0165802\mathcal{I}\left(R_7 R_8^*\right) + 0.00191257\mathcal{I}\left(R_7 R_9^*\right) + 0.0100512\mathcal{I}\left(R_8 R_9^*\right) \\
&- 0.000205119\mathcal{I}\left(R_8 R_{10}^*\right) + 0.0473551\mathcal{R}\left(R_7 R_8^*\right) - 0.322251\mathcal{R}\left(R_7 R_9^*\right) \\
&- 0.0334039\mathcal{R}\left(R_8 R_9^*\right) + 0.0058446\mathcal{R}\left(R_7 R_{10}^*\right) + 0.000628542\mathcal{R}\left(R_8 R_{10}^*\right) \\
&- 0.00991432\mathcal{R}\left(R_9 R_{10}^*\right) + 0.213553\left|R_7\right|^2 + 0.00236325\left|R_8\right|^2 \\
&+ 0.134982\left|R_9\right|^2 + 0.977388\left|R_{10}\right|^2 + 0.0384061\mathcal{I}\left(R_7\right) \\
&- 0.00817015\mathcal{I}\left(R_8\right) - 0.0252\mathcal{I}\left(R_9\right) + 0.000290922\mathcal{I}\left(R_{10}\right) \\
&+ 0.469276\mathcal{R}\left(R_7\right) + 0.0447868\mathcal{R}\left(R_8\right) - 0.276771\mathcal{R}\left(R_9\right) \\
&\left. - 0.0390521\mathcal{R}\left(R_{10}\right) + 0.269424\right] \times 10^{-7}\,, \tag{B.41}
\end{aligned}
$$

$$
\begin{aligned}
\mathcal{H}_T[3.5,6]_{\text{no em}} = &\Big[0.0053151\mathcal{I}\left(R_7 R_8^*\right) + 0.00144479\mathcal{I}\left(R_7 R_9^*\right) + 0.00759287\mathcal{I}\left(R_8 R_9^*\right) \\
&- 0.00015495\mathcal{I}\left(R_8 R_{10}^*\right) + 0.0152428\mathcal{R}\left(R_7 R_8^*\right) - 0.243575\mathcal{R}\left(R_7 R_9^*\right) \\
&- 0.0253318\mathcal{R}\left(R_8 R_9^*\right) + 0.0044113\mathcal{R}\left(R_7 R_{10}^*\right) + 0.000476328\mathcal{R}\left(R_8 R_{10}^*\right) \\
&- 0.0159082\mathcal{R}\left(R_9 R_{10}^*\right) + 0.0684719\left|R_7\right|^2 + 0.000762226\left|R_8\right|^2 \\
&+ 0.217119\left|R_9\right|^2 + 1.56931\left|R_{10}\right|^2 + 0.0180057\mathcal{I}\left(R_7\right) \\
&+ 0.00474718\mathcal{I}\left(R_8\right) - 0.0218638\mathcal{I}\left(R_9\right) + 0.000110893\mathcal{I}\left(R_{10}\right) \\
&- 0.135386\mathcal{R}\left(R_7\right) - 0.0137382\mathcal{R}\left(R_8\right) + 0.220517\mathcal{R}\left(R_9\right) \\
&\left. - 0.0757004\mathcal{R}\left(R_{10}\right) + 0.0549339\right] \times 10^{-7}\,, \tag{B.42}
\end{aligned}
$$

$$
\begin{aligned}
\mathcal{H}_T[1,6]_{\text{no em}} = &\Big[0.0218953\mathcal{I}\left(R_7 R_8^*\right) + 0.00335736\mathcal{I}\left(R_7 R_9^*\right) + 0.017644\mathcal{I}\left(R_8 R_9^*\right) \\
&- 0.00036007\mathcal{I}\left(R_8 R_{10}^*\right) + 0.0625979\mathcal{R}\left(R_7 R_8^*\right) - 0.565826\mathcal{R}\left(R_7 R_9^*\right) \\
&- 0.0587357\mathcal{R}\left(R_8 R_9^*\right) + 0.0102559\mathcal{R}\left(R_7 R_{10}^*\right) + 0.00110487\mathcal{R}\left(R_8 R_{10}^*\right) \\
&- 0.0258225\mathcal{R}\left(R_9 R_{10}^*\right) + 0.282025\left|R_7\right|^2 + 0.00312548\left|R_8\right|^2 \\
&+ 0.352102\left|R_9\right|^2 + 2.5467\left|R_{10}\right|^2 + 0.0564119\mathcal{I}\left(R_7\right) \\
&- 0.00342297\mathcal{I}\left(R_8\right) - 0.0470638\mathcal{I}\left(R_9\right) + 0.000401815\mathcal{I}\left(R_{10}\right)
\end{aligned}
$$

$$+ 0.33389\mathcal{R}\left(R_7\right) + 0.0310485\mathcal{R}\left(R_8\right) - 0.0562543\mathcal{R}\left(R_9\right)$$
$$- 0.114753\mathcal{R}\left(R_{10}\right) + 0.324358\Big] \times 10^{-7}. \tag{B.43}$$

B.6 $\mathcal{H}_3$ and $\mathcal{H}_4$

$$\mathcal{H}_3[1, 3.5]_{ee} = \Big[- 1.77941\mathcal{R}\left(R_7 R_{10}^*\right) - 0.134875\mathcal{R}\left(R_8 R_{10}^*\right) + 3.00277\mathcal{R}\left(R_9 R_{10}^*\right)$$
$$+ 0.0272335\mathcal{I}\left(R_{10}\right) + 3.15458\mathcal{R}\left(R_{10}\right) - 0.106259\Big] \times 10^{-9}, \tag{B.44}$$

$$\mathcal{H}_3[3.5, 6]_{ee} = \Big[- 0.933808\mathcal{R}\left(R_7 R_{10}^*\right) - 0.0707802\mathcal{R}\left(R_8 R_{10}^*\right) + 2.48483\mathcal{R}\left(R_9 R_{10}^*\right)$$
$$+ 0.136987\mathcal{I}\left(R_{10}\right) + 3.6078\mathcal{R}\left(R_{10}\right) - 0.0879303\Big] \times 10^{-9}, \tag{B.45}$$

$$\mathcal{H}_3[1, 6]_{ee} = \Big[- 2.71322\mathcal{R}\left(R_7 R_{10}^*\right) - 0.205655\mathcal{R}\left(R_8 R_{10}^*\right) + 5.48761\mathcal{R}\left(R_9 R_{10}^*\right)$$
$$+ 0.164221\mathcal{I}\left(R_{10}\right) + 6.76238\mathcal{R}\left(R_{10}\right) - 0.194189\Big] \times 10^{-9}, \tag{B.46}$$

$$\mathcal{H}_3[1, 3.5]_{\mu\mu} = \Big[- 0.739705\mathcal{R}\left(R_7 R_{10}^*\right) - 0.0560677\mathcal{R}\left(R_8 R_{10}^*\right) + 1.24826\mathcal{R}\left(R_9 R_{10}^*\right)$$
$$+ 0.011321\mathcal{I}\left(R_{10}\right) + 1.31401\mathcal{R}\left(R_{10}\right) - 0.0441719\Big] \times 10^{-9}, \tag{B.47}$$

$$\mathcal{H}_3[3.5, 6]_{\mu\mu} = \Big[- 0.388185\mathcal{R}\left(R_7 R_{10}^*\right) - 0.0294234\mathcal{R}\left(R_8 R_{10}^*\right) + 1.03295\mathcal{R}\left(R_9 R_{10}^*\right)$$
$$+ 0.0569458\mathcal{I}\left(R_{10}\right) + 1.50196\mathcal{R}\left(R_{10}\right) - 0.0365528\Big] \times 10^{-9}, \tag{B.48}$$

$$\mathcal{H}_3[1, 6]_{\mu\mu} = \Big[- 1.12789\mathcal{R}\left(R_7 R_{10}^*\right) - 0.0854912\mathcal{R}\left(R_8 R_{10}^*\right) + 2.28121\mathcal{R}\left(R_9 R_{10}^*\right)$$
$$+ 0.0682668\mathcal{I}\left(R_{10}\right) + 2.81597\mathcal{R}\left(R_{10}\right) - 0.0807247\Big] \times 10^{-9}, \tag{B.49}$$

$$\mathcal{H}_4[1, 3.5]_{ee} = \Big[0.013885\mathcal{R}\left(R_7 R_8^*\right) - 0.36974\mathcal{R}\left(R_7 R_9^*\right) - 0.0280253\mathcal{R}\left(R_8 R_9^*\right)$$
$$+ 0.0915928\left|R_7\right|^2 + 0.000526223\left|R_8\right|^2 + 0.493116\left|R_9\right|^2$$
$$+ 3.41677\left|R_{10}\right|^2 - 0.0427247\mathcal{I}\left(R_7\right) - 0.00323842\mathcal{I}\left(R_8\right)$$
$$+ 0.206797\mathcal{I}\left(R_9\right) - 0.44318\mathcal{R}\left(R_7\right) - 0.0349731\mathcal{R}\left(R_8\right)$$
$$+ 1.50448\mathcal{R}\left(R_9\right) + 1.72231\Big] \times 10^{-9}, \tag{B.50}$$

$$\mathcal{H}_4[3.5, 6]_{ee} = \Big[0.00356372\mathcal{R}\left(R_7 R_8^*\right) - 0.130439\mathcal{R}\left(R_7 R_9^*\right) - 0.00988691\mathcal{R}\left(R_8 R_9^*\right)$$
$$+ 0.0235082\left|R_7\right|^2 + 0.00013506\left|R_8\right|^2 + 0.183801\left|R_9\right|^2$$
$$+ 1.27355\left|R_{10}\right|^2 - 0.026613\mathcal{I}\left(R_7\right) - 0.00201719\mathcal{I}\left(R_8\right)$$
$$+ 0.13151\mathcal{I}\left(R_9\right) - 0.181082\mathcal{R}\left(R_7\right) - 0.0142128\mathcal{R}\left(R_8\right)$$
$$+ 0.541921\mathcal{R}\left(R_9\right) + 0.544544\Big] \times 10^{-9}, \tag{B.51}$$

$$\mathcal{H}_4[1, 6]_{ee} = \Big[0.0174487\mathcal{R}\left(R_7 R_8^*\right) - 0.500179\mathcal{R}\left(R_7 R_9^*\right) - 0.0379122\mathcal{R}\left(R_8 R_9^*\right)$$
$$+ 0.115101\left|R_7\right|^2 + 0.000661283\left|R_8\right|^2 + 0.676917\left|R_9\right|^2$$
$$+ 4.69032\left|R_{10}\right|^2 - 0.0693376\mathcal{I}\left(R_7\right) - 0.00525561\mathcal{I}\left(R_8\right)$$

$$+ 0.338308\mathcal{I}\left(R_9\right) - 0.624262\mathcal{R}\left(R_7\right) - 0.0491858\mathcal{R}\left(R_8\right)$$
$$+ 2.0464\mathcal{R}\left(R_9\right) + 2.26685\Big] \times 10^{-9}\,, \tag{B.52}$$

$$\mathcal{H}_4[1,3.5]_{\mu\mu} = \Big[0.00577201\mathcal{R}\left(R_7 R_8^*\right) - 0.153702\mathcal{R}\left(R_7 R_9^*\right) - 0.0116502\mathcal{R}\left(R_8 R_9^*\right)$$
$$+ 0.0380753\left|R_7\right|^2 + 0.000218752\left|R_8\right|^2 + 0.204989\left|R_9\right|^2$$
$$+ 1.42036\left|R_{10}\right|^2 - 0.0177607\mathcal{I}\left(R_7\right) - 0.00134622\mathcal{I}\left(R_8\right)$$
$$+ 0.085966\mathcal{I}\left(R_9\right) - 0.184556\mathcal{R}\left(R_7\right) - 0.014563\mathcal{R}\left(R_8\right)$$
$$+ 0.626285\mathcal{R}\left(R_9\right) + 0.717523\Big] \times 10^{-9}\,, \tag{B.53}$$

$$\mathcal{H}_4[3.5,6]_{\mu\mu} = \Big[0.00148144\mathcal{R}\left(R_7 R_8^*\right) - 0.0542236\mathcal{R}\left(R_7 R_9^*\right) - 0.00411001\mathcal{R}\left(R_8 R_9^*\right)$$
$$+ 0.00977239\left|R_7\right|^2 + 0.0000561448\left|R_8\right|^2 + 0.0764064\left|R_9\right|^2$$
$$+ 0.529415\left|R_{10}\right|^2 - 0.0110631\mathcal{I}\left(R_7\right) - 0.000838551\mathcal{I}\left(R_8\right)$$
$$+ 0.0546691\mathcal{I}\left(R_9\right) - 0.0753908\mathcal{R}\left(R_7\right) - 0.00591698\mathcal{R}\left(R_8\right)$$
$$+ 0.225601\mathcal{R}\left(R_9\right) + 0.22693\Big] \times 10^{-9}\,, \tag{B.54}$$

$$\mathcal{H}_4[1,6]_{\mu\mu} = \Big[0.00725346\mathcal{R}\left(R_7 R_8^*\right) - 0.207925\mathcal{R}\left(R_7 R_9^*\right) - 0.0157602\mathcal{R}\left(R_8 R_9^*\right)$$
$$+ 0.0478477\left|R_7\right|^2 + 0.000274897\left|R_8\right|^2 + 0.281396\left|R_9\right|^2$$
$$+ 1.94977\left|R_{10}\right|^2 - 0.0288238\mathcal{I}\left(R_7\right) - 0.00218477\mathcal{I}\left(R_8\right)$$
$$+ 0.140635\mathcal{I}\left(R_9\right) - 0.259947\mathcal{R}\left(R_7\right) - 0.02048\mathcal{R}\left(R_8\right)$$
$$+ 0.851886\mathcal{R}\left(R_9\right) + 0.944453\Big] \times 10^{-9}\,, \tag{B.55}$$

References

[1] BaBar and Belle collaborations, *The physics of the B factories*, *Eur. Phys. J. C* **74** (2014) 3026 [[arXiv:1406.6311](#)] [INSPIRE].

[2] CDF collaboration, *Measurements of the angular distributions in the decays $B \to K^{(*)}\mu^+\mu^-$ at CDF*, *Phys. Rev. Lett.* **108** (2012) 081807 [[arXiv:1108.0695](#)] [INSPIRE].

[3] BaBar collaboration, *Measurement of angular asymmetries in the decays $B \to K^*\ell^+\ell^-$*, *Phys. Rev. D* **93** (2016) 052015 [[arXiv:1508.07960](#)] [INSPIRE].

[4] Belle collaboration, *Lepton-flavor-dependent angular analysis of $B \to K^*\ell^+\ell^-$*, *Phys. Rev. Lett.* **118** (2017) 111801 [[arXiv:1612.05014](#)] [INSPIRE].

[5] CMS collaboration, *Measurement of angular parameters from the decay $B^0 \to K^{*0}\mu^+\mu^-$ in proton-proton collisions at $\sqrt{s} = 8$ TeV*, *Phys. Lett. B* **781** (2018) 517 [[arXiv:1710.02846](#)] [INSPIRE].

[6] LHCb collaboration, *Test of lepton universality with $B^0 \to K^{*0}\ell^+\ell^-$ decays*, *JHEP* **08** (2017) 055 [[arXiv:1705.05802](#)] [INSPIRE].

[7] ATLAS collaboration, *Angular analysis of $B_d^0 \to K^* \mu^+ \mu^-$ decays in pp collisions at $\sqrt{s} = 8$ TeV with the ATLAS detector*, *JHEP* **10** (2018) 047 [arXiv:1805.04000] [INSPIRE].

[8] BELLE collaboration, *Test of lepton flavor universality in $B \to K^* \ell^+ \ell^-$ decays at Belle*, arXiv:1904.02440 [INSPIRE].

[9] LHCb collaboration, *Search for lepton-universality violation in $B^+ \to K^+ \ell^+ \ell^-$ decays*, *Phys. Rev. Lett.* **122** (2019) 191801 [arXiv:1903.09252] [INSPIRE].

[10] LHCb collaboration, *Measurement of CP-averaged observables in the $B^0 \to K^{*0} \mu^+ \mu^-$ decay*, *Phys. Rev. Lett.* **125** (2020) 011802 [arXiv:2003.04831] [INSPIRE].

[11] F. Beaujean, C. Bobeth and D. van Dyk, *Comprehensive Bayesian analysis of rare (semi)leptonic and radiative B decays*, *Eur. Phys. J. C* **74** (2014) 2897 [*Erratum ibid.* **74** (2014) 3179] [arXiv:1310.2478] [INSPIRE].

[12] G. Hiller and M. Schmaltz, *R_K and future $b \to s\ell\ell$ physics beyond the Standard Model opportunities*, *Phys. Rev. D* **90** (2014) 054014 [arXiv:1408.1627] [INSPIRE].

[13] S. Descotes-Genon, L. Hofer, J. Matias and J. Virto, *Global analysis of $b \to s\ell\ell$ anomalies*, *JHEP* **06** (2016) 092 [arXiv:1510.04239] [INSPIRE].

[14] M. Bordone, G. Isidori and A. Pattori, *On the Standard Model predictions for R_K and R_{K^*}*, *Eur. Phys. J. C* **76** (2016) 440 [arXiv:1605.07633] [INSPIRE].

[15] G. D'Amico et al., *Flavour anomalies after the R_{K^*} measurement*, *JHEP* **09** (2017) 010 [arXiv:1704.05438] [INSPIRE].

[16] W. Altmannshofer, P. Stangl and D.M. Straub, *Interpreting hints for lepton flavor universality violation*, *Phys. Rev. D* **96** (2017) 055008 [arXiv:1704.05435] [INSPIRE].

[17] M. Ciuchini et al., *On flavourful easter eggs for new physics hunger and lepton flavour universality violation*, *Eur. Phys. J. C* **77** (2017) 688 [arXiv:1704.05447] [INSPIRE].

[18] B. Capdevila, A. Crivellin, S. Descotes-Genon, J. Matias and J. Virto, *Patterns of new physics in $b \to s\ell^+\ell^-$ transitions in the light of recent data*, *JHEP* **01** (2018) 093 [arXiv:1704.05340] [INSPIRE].

[19] M. Algueró et al., *Emerging patterns of new physics with and without lepton flavour universal contributions*, *Eur. Phys. J. C* **79** (2019) 714 [*Addendum ibid.* **80** (2020) 511] [arXiv:1903.09578] [INSPIRE].

[20] T. Hurth, F. Mahmoudi and S. Neshatpour, *Implications of the new LHCb angular analysis of $B \to K^* \mu^+ \mu^-$: hadronic effects or new physics?*, *Phys. Rev. D* **102** (2020) 055001 [arXiv:2006.04213] [INSPIRE].

[21] BELLE-II collaboration, *The Belle II physics book*, *PTEP* **2019** (2019) 123C01 [*Erratum ibid.* **2020** (2020) 029201] [arXiv:1808.10567] [INSPIRE].

[22] M. Misiak, *The $b \to s e^+ e^-$ and $b \to s\gamma$ decays with next-to-leading logarithmic QCD corrections*, *Nucl. Phys. B* **393** (1993) 23 [*Erratum ibid.* **439** (1995) 461] [INSPIRE].

[23] A.J. Buras and M. Münz, *Effective Hamiltonian for $B \to X_s e^+ e^-$ beyond leading logarithms in the NDR and HV schemes*, *Phys. Rev. D* **52** (1995) 186 [hep-ph/9501281] [INSPIRE].

[24] C. Bobeth, M. Misiak and J. Urban, *Photonic penguins at two loops and m_t dependence of $BR[B \to X_s \ell^+ \ell^-]$*, *Nucl. Phys. B* **574** (2000) 291 [hep-ph/9910220] [INSPIRE].

[25] P. Gambino, M. Gorbahn and U. Haisch, *Anomalous dimension matrix for radiative and rare semileptonic B decays up to three loops*, *Nucl. Phys. B* **673** (2003) 238 [hep-ph/0306079] [INSPIRE].

[26] M. Gorbahn and U. Haisch, *Effective Hamiltonian for non-leptonic $|\Delta F| = 1$ decays at NNLO in QCD*, *Nucl. Phys. B* **713** (2005) 291 [hep-ph/0411071] [INSPIRE].

[27] H.H. Asatryan, H.M. Asatrian, C. Greub and M. Walker, *Calculation of two loop virtual corrections to $b \to s\ell^+\ell^-$ in the Standard Model*, *Phys. Rev. D* **65** (2002) 074004 [hep-ph/0109140] [INSPIRE].

[28] H.H. Asatrian, H.M. Asatrian, C. Greub and M. Walker, *Two loop virtual corrections to $B \to X_s\ell^+\ell^-$ in the Standard Model*, *Phys. Lett. B* **507** (2001) 162 [hep-ph/0103087] [INSPIRE].

[29] H.H. Asatryan, H.M. Asatrian, C. Greub and M. Walker, *Complete gluon bremsstrahlung corrections to the process $b \to s\ell^+\ell^-$*, *Phys. Rev. D* **66** (2002) 034009 [hep-ph/0204341] [INSPIRE].

[30] A. Ghinculov, T. Hurth, G. Isidori and Y.P. Yao, *Forward backward asymmetry in $B \to X_s\ell^+\ell^-$ at the NNLL level*, *Nucl. Phys. B* **648** (2003) 254 [hep-ph/0208088] [INSPIRE].

[31] H.M. Asatrian, K. Bieri, C. Greub and A. Hovhannisyan, *NNLL corrections to the angular distribution and to the forward backward asymmetries in $B \to X_s\ell^+\ell^-$*, *Phys. Rev. D* **66** (2002) 094013 [hep-ph/0209006] [INSPIRE].

[32] H.M. Asatrian, H.H. Asatryan, A. Hovhannisyan and V. Poghosyan, *Complete bremsstrahlung corrections to the forward backward asymmetries in $b \to X_s\ell^+\ell^-$*, *Mod. Phys. Lett. A* **19** (2004) 603 [hep-ph/0311187] [INSPIRE].

[33] A. Ghinculov, T. Hurth, G. Isidori and Y.P. Yao, *New NNLL results on the decay $B \to X_s\ell^+\ell^-$*, *Eur. Phys. J. C* **33** (2004) S288 [hep-ph/0310187] [INSPIRE].

[34] A. Ghinculov, T. Hurth, G. Isidori and Y.P. Yao, *The rare decay $B \to X_s\ell^+\ell^-$ to NNLL precision for arbitrary dilepton invariant mass*, *Nucl. Phys. B* **685** (2004) 351 [hep-ph/0312128] [INSPIRE].

[35] C. Greub, V. Pilipp and C. Schupbach, *Analytic calculation of two-loop QCD corrections to $b \to s\ell^+\ell^-$ in the high q^2 region*, *JHEP* **12** (2008) 040 [arXiv:0810.4077] [INSPIRE].

[36] C. Bobeth, P. Gambino, M. Gorbahn and U. Haisch, *Complete NNLO QCD analysis of $\bar{B} \to X_s\ell^+\ell^-$ and higher order electroweak effects*, *JHEP* **04** (2004) 071 [hep-ph/0312090] [INSPIRE].

[37] S. de Boer, *Two loop virtual corrections to $b \to (d, s)\ell^+\ell^-$ and $c \to u\ell^+\ell^-$ for arbitrary momentum transfer*, *Eur. Phys. J. C* **77** (2017) 801 [arXiv:1707.00988] [INSPIRE].

[38] T. Huber, E. Lunghi, M. Misiak and D. Wyler, *Electromagnetic logarithms in $\bar{B} \to X_s\ell^+\ell^-$*, *Nucl. Phys. B* **740** (2006) 105 [hep-ph/0512066] [INSPIRE].

[39] T. Huber, T. Hurth and E. Lunghi, *Logarithmically enhanced corrections to the decay rate and forward backward asymmetry in $\bar{B} \to X_s\ell^+\ell^-$*, *Nucl. Phys. B* **802** (2008) 40 [arXiv:0712.3009] [INSPIRE].

[40] T. Huber, T. Hurth and E. Lunghi, *Inclusive $\bar{B} \to X_s\ell^+\ell^-$: complete angular analysis and a thorough study of collinear photons*, *JHEP* **06** (2015) 176 [arXiv:1503.04849] [INSPIRE].

[41] T. Huber, Q. Qin and K.K. Vos, *Five-particle contributions to the inclusive rare* $\bar{B} \to X_{s(d)}\ell^+\ell^-$ *decays*, *Eur. Phys. J. C* **78** (2018) 748 [arXiv:1806.11521] [INSPIRE].

[42] A.F. Falk, M.E. Luke and M.J. Savage, *Nonperturbative contributions to the inclusive rare decays* $B \to X_s\gamma$ *and* $B \to X_s\ell^+\ell^-$, *Phys. Rev. D* **49** (1994) 3367 [hep-ph/9308288] [INSPIRE].

[43] A. Ali, G. Hiller, L.T. Handoko and T. Morozumi, *Power corrections in the decay rate and distributions in* $B \to X_s\ell^+\ell^-$ *in the Standard Model*, *Phys. Rev. D* **55** (1997) 4105 [hep-ph/9609449] [INSPIRE].

[44] J.-W. Chen, G. Rupak and M.J. Savage, *Non-$1/m_b^n$ power suppressed contributions to inclusive* $B \to X_s\ell^+\ell^-$ *decays*, *Phys. Lett. B* **410** (1997) 285 [hep-ph/9705219] [INSPIRE].

[45] G. Buchalla and G. Isidori, *Nonperturbative effects in* $\bar{B} \to X_s\ell^+\ell^-$ *for large dilepton invariant mass*, *Nucl. Phys. B* **525** (1998) 333 [hep-ph/9801456] [INSPIRE].

[46] C.W. Bauer and C.N. Burrell, *Nonperturbative corrections to moments of the decay* $B \to X_s\ell^+\ell^-$, *Phys. Rev. D* **62** (2000) 114028 [hep-ph/9911404] [INSPIRE].

[47] Z. Ligeti and F.J. Tackmann, *Precise predictions for* $B \to X_s\ell^+\ell^-$ *in the large q^2 region*, *Phys. Lett. B* **653** (2007) 404 [arXiv:0707.1694] [INSPIRE].

[48] F. Krüger and L.M. Sehgal, *Lepton polarization in the decays* $b \to X_s\mu^+\mu^-$ *and* $B \to X_s\tau^+\tau^-$, *Phys. Lett. B* **380** (1996) 199 [hep-ph/9603237] [INSPIRE].

[49] F. Krüger and L.M. Sehgal, *CP violation in the decay* $B \to X_d e^+e^-$, *Phys. Rev. D* **55** (1997) 2799 [hep-ph/9608361] [INSPIRE].

[50] T. Huber, T. Hurth, J. Jenkins, E. Lunghi, Q. Qin and K.K. Vos, *Long distance effects in inclusive rare B decays and phenomenology of* $\bar{B} \to X_d\ell^+\ell^-$, *JHEP* **10** (2019) 228 [arXiv:1908.07507] [INSPIRE].

[51] T. Hurth, M. Fickinger, S. Turczyk and M. Benzke, *Resolved power corrections to the inclusive decay* $\bar{B} \to X_s\ell^+\ell^-$, *Nucl. Part. Phys. Proc.* **285-286** (2017) 57 [arXiv:1711.01162] [INSPIRE].

[52] M. Benzke, T. Hurth and S. Turczyk, *Subleading power factorization in* $\bar{B} \to X_s\ell^+\ell^-$, *JHEP* **10** (2017) 031 [arXiv:1705.10366] [INSPIRE].

[53] M. Benzke and T. Hurth, *Resolved $1/m_b$ contributions to* $b \to s\ell\ell$ *and* $b \to s\gamma$, arXiv:2006.00624 [INSPIRE].

[54] M.B. Voloshin, *Large $O(m_c^{-2})$ nonperturbative correction to the inclusive rate of the decay* $B \to X_s\gamma$, *Phys. Lett. B* **397** (1997) 275 [hep-ph/9612483] [INSPIRE].

[55] G. Buchalla, G. Isidori and S.J. Rey, *Corrections of order $\Lambda_{\rm QCD}^2/m_c^2$ to inclusive rare B decays*, *Nucl. Phys. B* **511** (1998) 594 [hep-ph/9705253] [INSPIRE].

[56] K.S.M. Lee, Z. Ligeti, I.W. Stewart and F.J. Tackmann, *Extracting short distance information from* $b \to s\ell^+\ell^-$ *effectively*, *Phys. Rev. D* **75** (2007) 034016 [hep-ph/0612156] [INSPIRE].

[57] K.S.M. Lee and I.W. Stewart, *Shape-function effects and split matching in* $B \to X_s\ell^+\ell^-$, *Phys. Rev. D* **74** (2006) 014005 [hep-ph/0511334] [INSPIRE].

[58] K.S.M. Lee, Z. Ligeti, I.W. Stewart and F.J. Tackmann, *Universality and m_X cut effects in* $B \to X_s\ell^+\ell^-$, *Phys. Rev. D* **74** (2006) 011501 [hep-ph/0512191] [INSPIRE].

[59] K.S.M. Lee and F.J. Tackmann, *Nonperturbative m_X cut effects in $B \to X_s \ell^+ \ell^-$ observables*, *Phys. Rev. D* **79** (2009) 114021 [arXiv:0812.0001] [INSPIRE].

[60] G. Bell, M. Beneke, T. Huber and X.-Q. Li, *Heavy-to-light currents at NNLO in SCET and semi-inclusive $\bar{B} \to X_s \ell^+ \ell^-$ decay*, *Nucl. Phys. B* **843** (2011) 143 [arXiv:1007.3758] [INSPIRE].

[61] M.B. Voloshin, *Nonfactorization effects in heavy mesons and determination of $|V_{ub}|$ from inclusive semileptonic B decays*, *Phys. Lett. B* **515** (2001) 74 [hep-ph/0106040] [INSPIRE].

[62] CLEO collaboration, *Measurement of absolute branching fractions of inclusive semileptonic decays of charm and charmed-strange mesons*, *Phys. Rev. D* **81** (2010) 052007 [arXiv:0912.4232] [INSPIRE].

[63] P. Gambino and J.F. Kamenik, *Lepton energy moments in semileptonic charm decays*, *Nucl. Phys. B* **840** (2010) 424 [arXiv:1004.0114] [INSPIRE].

[64] CKMFITTER GROUP collaboration, *CP violation and the CKM matrix: assessing the impact of the asymmetric B factories*, *Eur. Phys. J. C* **41** (2005) 1 [hep-ph/0406184] [INSPIRE].

[65] HEAVY FLAVOR AVERAGING GROUP collaboration, *Averages of B-hadron, C-hadron, and τ-lepton properties as of early* 2012, arXiv:1207.1158 [INSPIRE].

[66] C. Schwanda, *Determination of $|V_{cb}|$ from inclusive decays $B \to X_c \ell \nu$ using a global fit*, in 7$^{\text{th}}$ *international workshop on the CKM unitarity triangle*, (2013) [arXiv:1302.0294] [INSPIRE].

[67] HFLAV collaboration, *Averages of b-hadron, c-hadron and τ-lepton properties as of summer* 2016, *Eur. Phys. J. C* **77** (2017) 895 [arXiv:1612.07233] [INSPIRE].

[68] A. Alberti, P. Gambino, K.J. Healey and S. Nandi, *Precision determination of the Cabibbo-Kobayashi-Maskawa element V_{cb}*, *Phys. Rev. Lett.* **114** (2015) 061802 [arXiv:1411.6560] [INSPIRE].

[69] P. Gambino, K.J. Healey and S. Turczyk, *Taming the higher power corrections in semileptonic B decays*, *Phys. Lett. B* **763** (2016) 60 [arXiv:1606.06174] [INSPIRE].

[70] PARTICLE DATA GROUP collaboration, *Review of particle physics*, *Phys. Rev. D* **98** (2018) 030001 [INSPIRE].

[71] D.J. Lange, *The EvtGen particle decay simulation package*, *Nucl. Instrum. Meth. A* **462** (2001) 152 [INSPIRE].

[72] T. Sjöstrand, *High-energy physics event generation with PYTHIA 5.7 and JETSET 7.4*, *Comput. Phys. Commun.* **82** (1994) 74 [INSPIRE].

[73] P. Golonka and Z. Was, *PHOTOS Monte Carlo: a precision tool for QED corrections in Z and W decays*, *Eur. Phys. J. C* **45** (2006) 97 [hep-ph/0506026] [INSPIRE].

[74] BABAR collaboration, *Measurement of the $B \to X_s \ell^+ \ell^-$ branching fraction with a sum over exclusive modes*, *Phys. Rev. Lett.* **93** (2004) 081802 [hep-ex/0404006] [INSPIRE].

[75] BABAR collaboration, *Measurement of the $B \to X_s \ell^+ \ell^-$ branching fraction and search for direct CP-violation from a sum of exclusive final states*, *Phys. Rev. Lett.* **112** (2014) 211802 [arXiv:1312.5364] [INSPIRE].

[76] BELLE collaboration, *Improved measurement of the electroweak penguin process $B \to X_s \ell^+ \ell^-$*, *Phys. Rev. D* **72** (2005) 092005 [hep-ex/0503044] [INSPIRE].

[77] BELLE collaboration, *Measurement of the lepton forward-backward asymmetry in* $B \to X_s \ell^+ \ell^-$ *decays with a sum of exclusive modes*, *Phys. Rev. D* **93** (2016) 032008 [*Addendum ibid.* **93** (2016) 059901] [arXiv:1402.7134] [INSPIRE].

[78] T. Hurth, *Inclusive semi-leptonic penguin decays*, in *XXIV Cracow EPIPHANY conference on advances in heavy flavor physics*, Cracow, Poland, 9–10 January 2018.

[79] P. Gambino, P. Giordano, G. Ossola and N. Uraltsev, *Inclusive semileptonic B decays and the determination of* $|V_{ub}|$, *JHEP* **10** (2007) 058 [arXiv:0707.2493] [INSPIRE].

[80] D.M. Straub, *flavio: a python package for flavour and precision phenomenology in the Standard Model and beyond*, arXiv:1810.08132 [INSPIRE].

[81] J. Aebischer, J. Kumar, P. Stangl and D.M. Straub, *A global likelihood for precision constraints and flavour anomalies*, *Eur. Phys. J. C* **79** (2019) 509 [arXiv:1810.07698] [INSPIRE].

[82] C. Bobeth, M. Gorbahn, T. Hermann, M. Misiak, E. Stamou and M. Steinhauser, $B_{s,d} \to \ell^+ \ell^-$ *in the Standard Model with reduced theoretical uncertainty*, *Phys. Rev. Lett.* **112** (2014) 101801 [arXiv:1311.0903] [INSPIRE].

[83] A. Cerri et al., *Report from working group 4: opportunities in flavour physics at the HL-LHC and HE-LHC*, in *Report on the physics at the HL-LHC and perspectives for the HE-LHC*, volume 7, A. Dainese et al. eds., (2019), pg. 867 [arXiv:1812.07638] [INSPIRE].

[84] BABAR collaboration, *Search for* $B^+ \to K^+ \tau^+ \tau^-$ *at the BaBar experiment*, *Phys. Rev. Lett.* **118** (2017) 031802 [arXiv:1605.09637] [INSPIRE].

[85] LHCb collaboration, *Search for the decays* $B_s^0 \to \tau^+ \tau^-$ *and* $B^0 \to \tau^+ \tau^-$, *Phys. Rev. Lett.* **118** (2017) 251802 [arXiv:1703.02508] [INSPIRE].

[86] C. Cornella, G. Isidori, M. König, S. Liechti, P. Owen and N. Serra, *Hunting for* $B^+ \to K^+ \tau^+ \tau^-$ *imprints on the* $B^+ \to K^+ \mu^+ \mu^-$ *dimuon spectrum*, arXiv:2001.04470 [INSPIRE].